

# **EFFECT OF ADDITIVES ON SINTERING OF $Ti_3SiC_2$ POWDER**

**A Dissertation Submitted  
in Partial Fulfillment of the Requirements for  
The Degree of Master of Technology**

**By  
Rahul Bapurao Mane**

**Under the Supervision of  
Dr. Bharat B. Panigrahi**



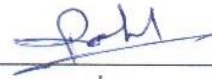
भारतीय प्रौद्योगिकी संस्थान हैदराबाद  
Indian Institute of Technology Hyderabad

**Department of Materials Science & Metallurgical Engineering  
Indian Institute of Technology Hyderabad**

**July, 2014**

## Declaration

I declare that this written submission represents my ideas in my own words and where others' ideas or words have been included, I have adequately cited and referenced the original sources. I also declare that I have adhered to all principles of academic honesty and integrity and have not misrepresented or fabricated or falsified any idea/data/fact/source in my submission. I understand that any violation of the above will be a cause for disciplinary action by the Institute and can also evoke penal action from the sources that have thus not been properly cited, or from whom proper permission has not been taken when needed.

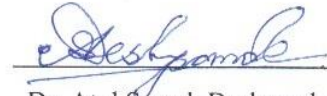


Rahul Bapurao Mane

MS12M1006

## Approval Sheet

This thesis entitled *Effect of additives on sintering of  $Ti_3SiC_2$  powder* by Rahul Bapurao Mane is approved for the degree of Master of Technology from IIT Hyderabad.



Dr. Atul Suresh Deshpande

Assistant Professor Dept. of MSME

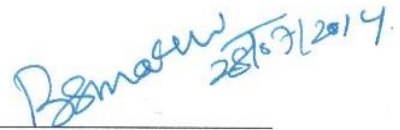
Examiner



Dr. Bharat Bhooshan Panigrahi

Assistant Professor Dept. of MSME

Supervisor



Dr. Bhabani Shankar Mallik

Assistant Professor Dept. of Chemistry

Chairman

## **Acknowledgements**

I am extremely indebted a lot to my supervisor Dr. Bharat Bhooshan Panigrahi, Assistant professor Department of Material Science & Metallurgical Engineering, IIT Hyderabad for his excellent guidance, constructive criticism, valuable suggestions, encouragement and support throughout the research work. I am thankful of him for giving me opportunity to work with him.

I want to thank Dr. Pinaki Bhattacharjee Head of the Department of Material Science & Metallurgical Engineering, IIT Hyderabad and my entire faculty for giving world class education. I would like to show my sincere thanks to all Research scholars of Department of Material Science & Metallurgical Engineering, IIT Hyderabad. Specially Mr. Rajkumar, Mr. Akki, Mr. Damodar, Mr. Dan, Mrs. Sushamita, Mr. Zaid. For helping me to complete my experiments and sharing their knowledge.

I would also like to thank my friends who helped me lot and being a motivational source for me, special thanks to Mr. Ankit Joshi, Mr. Tushar Jogi, Mr. Bhalchandra Bhadak. Last but not least I would like to pay my high regards to my Aai Mrs. Sushama Bapurao Mane, who shouldered all the family responsibilities. I am grateful to my sister Mrs. Supriya Shrikant Punekar for her support along with consistent encouragement for my studies in difficult times.

Dedicated  
To  
My Father  
Appa  
Late, Bapurao Dnyandeo Mane

## **Abstract**

TSC has a potential for high temperature applications. For high temperature structural application, parts with good strength & oxidation resistance materials are always desirable. The aim of the present study is to produce high purity TSC powder, high density parts of TSC by using pressureless sintering, with some sintering aids like Si, Ni etc. Effects of sintering aid on sintering kinetics have been studied. This work attempts to study the sintering mechanism of TSC compound using dilatometer experiments under pressureless condition, Diffusion parameters, such as coefficient of diffusion and activation energy have been estimated. The present investigation focused on the non-isothermal sintering as well as isothermal sintering behavior. Activation energy for densification during non-isothermal heating was calculated using Young and Cutler's equation for different sintering mechanisms, it was observed that the values of activation energies increases with addition of sintering aids (Nickel). The Johnson Model was used for isothermal sintering study for TSC samples. Grain boundary diffusion coefficient and volume diffusion coefficient were calculated with the function of particle size and time.

**Keywords:** MAX phase, sintering, activation energy, diffusion, sintering aids.

# Contents

Declaration.....	2
Approval Sheet.....	3
Acknowledgements.....	4
Abstract.....	6
1 Introduction.....	8
2 Literature Review.....	10
2.1 Objectives.....	17
3 Experimental Procedure.....	18
3.1 Synthesis.....	18
3.2 Sintering.....	19
3.3 Dilatometry.....	21
3.4 Characterization.....	22
4 Results and Discussion.....	24
5 Conclusions.....	47
6 References.....	48

# Chapter 1

## Introduction

MAX phases are ternary carbides or Nitrides having  $M_{n+1}AX_n$  as general formula, where 'M' is early transition element from periodic table, 'A' is A group element, mostly they are IIIA and IVA group elements and 'X' is carbon or nitrogen. MAX phases have layered Hexagonal crystal structure and depending upon the value of n it can be called, 312, 413 materials [1]. It has unique combination of properties of metal and ceramics and the main reason for growing interest in the MAX phases lies in their unusual and sometimes unique set of properties, which makes them suitable for structural as well as functional application. Major difference between binary ceramics and MAX phase material is that MAX phase compounds basal dislocations numerous multiply and are mobile at room temperature as well as at high temperatures, where as in typical ceramic the number of slip system is zero at room temperature [2]. The ductility increases with increasing temperature.  $Ti_3SiC_2$ ,  $Ti_3AlC_2$ ,  $Ti_3GeC_2$ ,  $Cr_2AlC$ ,  $Ti_2AlC$  are the most studied MAX phase compounds. Before 2004, more than 50  $M_2AX$  (211 phase) compounds were determined. However, there are only three  $M_3AX_2$  compounds ( $Ti_3SiC_2$ ,  $Ti_3AlC_2$ ,  $Ti_3GeC_2$ ) and one  $M_4AX_3$  compound ( $Ti_4AlN_3$ ) [1, 3]. There are several new phases which might be stable due to the stable crystal structure of single cell, such as  $Ti_4AlC_3$ ,  $V_4SiC_3$ , and  $Ti_4SiN_3$ , however, to date; these phases could not be factually fabricated in experiments.

Crystal structure of  $Ti_3SiC_2$  (TSC) is shown in Fig 1.1.  $Ti_3SiC_2$  MAX phase material comes under 312 phase hexagonal crystal structure, at one layer of titanium, silicon and carbon is nearest atoms and at other layer of Ti on both sides only carbon layers are present. Every fourth layer is Si atoms layer and carbon is located at octahedral sites [5]. It has low density, high melting point, high young modulus, excellent thermal shock resistance, high electrical and thermal conductivities, good machinability, fracture toughness, good damage tolerance [2]. Damage tolerance is ability to resists the fracture from the preexistent cracks for a given period of time and is an essential



attribute of components, whose failure could result in catastrophic loss of life or property. The damage tolerance starts where the safe life ends. If we compare the properties of few selected MAX phase compound, most significant compound is TSC.

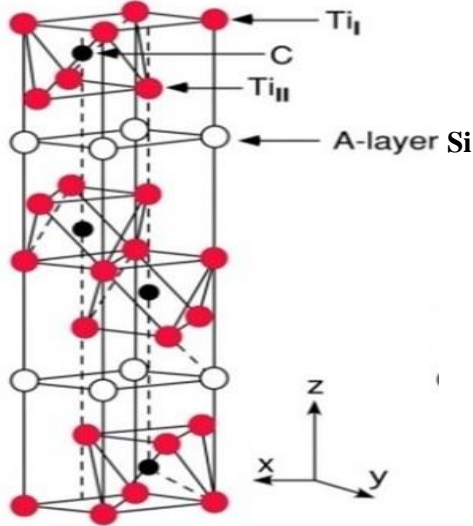


Figure1.1 Crystal structure of  $Ti_3SiC_2$  [5]

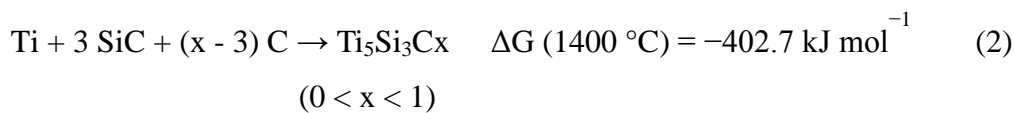
## Chapter 2

# Literature Review

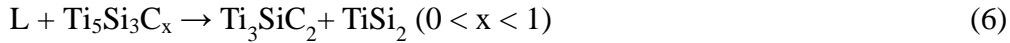
TiC is the most widely studied compound in MAX phase group which is produced using various combination of raw materials, like elemental powder synthesis [7], TiC+Si and TiC+SiC [1] etc . TiC was first synthesized by Jeitschko & Nowotny via chemical reaction, later it was produced through different synthesis routes [1]. There was difficulty in producing single phase TiC synthesis due to the very narrow region in the Ti-Si-C ternary diagram (Figure 2.1). Solid state reaction between  $TiC_{0.67}$  and Si reported to yield  $TiC_{0.67}$ , with low amount of TiC and intermetallic impurities. To produce high purity TiC phase excess amount of Si was used and small amounts of Al and  $B_2O_3$  were found to enhance the purity of TiC phase. It was reported that, at  $1300^{\circ}C$ , about 83% TiC phase was obtained after addition of sintering aid of  $B_2O_3$ . The mutual combustion reaction between elemental powders of Ti, Si, & C can be avoided by using  $B_2O_3$  and hence the binary phase impurity can be minimized. It was reported that, synthesis temperature was decreased with addition of aluminum (Al) and sintering temperature was decreased for single phase TiC. Addition of Al helped to control the decomposition of TiC phase. Al served as melting pool during sintering. It was reported that, during the sintering of TiC from Ti/SiC/C powder mixture, twin boundary energy of TiC was reduced effectively using Al. It was also reported that too much Al leads to the formation of aluminum related compound such as  $Ti_3AlC_2$  etc. It was reported that TiC, SiC and intermetallics were common impurities in TiC synthesis process [7-11]. Depending upon starting material different synthesis processes are used like direct synthesis of elemental powders and two stage synthesis processes where carbide is prepared first and then Si is added in second stage. The DSC analysis of mixed  $TiC_{0.67}$  and Si powder reported that exothermic nature of reaction during process. At  $800^{\circ}C$  reaction was started and it was observed that huge peak at  $985^{\circ}C$  and followed by number of small peaks were observed. The peak at  $985^{\circ}C$  represents major reaction and other peaks represent by-product formation. Before synthesis ball milling of mixed powders were done to obtain ultrafine powders [9]. Li et al. [13] have found that TiC,  $Ti_5Si_3$  and  $TiSi_2$  phases in the samples synthesized from

elemental powders. Silicon content is the main factor that determines the phase composition of the final products. Yang et al [10] reported the studies are the effect of varying silicon content in Ti/Si/TiC reactant mixture and concluded that the optimum silicon content should exceed the stoichiometric composition by about 10 wt%. They mentioned that excess silicon, compensated for Si loss by evaporation [10]. On the other hand too much Si increased undesired titanium silicides formation. By some authors TSC was also synthesized from TiC/Si powder mixtures, thus avoiding the use of pure titanium. Radhakrishnan et al. [7] reported that a reaction of 3TiC/2Si powders firstly generated TiSi<sub>2</sub> intermediate phase at a temperature of 1170 °C. In a second step it was converted to TSC where SiC was formed simultaneously. It was also reported that TSC was thermodynamically stable up to 1600 °C in vacuum for 24 hr. Decomposition of TSC was due to the presence of impurities [3]. Phase stability of MAX phases depends on their constitutive elements, atmosphere and the vapor pressure of the elements. For TSC system it was reported that, thin films decompose at lower temperature in comparison to the bulk TSC [3]. It has been reported that Self-propagating high temperature synthesis was not giving TSC phase for 1Ti+2TiC+1.1Si composition, because powder mixture highly stable TiC needs a lot of time at high temperature to react with other elements. TSC was obtained by SHS reaction with the maximum content of 88% and 86% from 3Ti+1.2SiC+0.8C and 3Ti+1.3Si+2C reactant mixtures respectively. The simultaneous formation of some intermediate phases such as TiC and TiSi<sub>2</sub> were detected [32].

Reaction mechanisms of TSC system were reported in some literatures. At the temperatures below 1400 °C, about five different reactions were observed for the reactant mixture of Ti, SiC and Graphite powder, as shown from eq. (1) to (5).



According to Eq. (5), free Si atoms can be formed during the sintering at high temperature. It was observed from Ti–Si–C phase diagram; liquid phase was appeared at above 1485 °C [35].



Where L = liquid phase,  $\Delta G$  = Gibbs free energy.

The high density parts of TSC were produced through the hot pressing, self-propagating high temperature synthesis process and pulse discharge sintering. Recently, Barsoum et al. made a great contribution to the synthesis and characterization on this material. They were successful in sintering of TSC through the hot isotactic pressing, while obtaining 80-90% of phase purity, with other unwanted phase of TiC [26]. High density of TSC was produced by using elemental mixtures as starting powder through HIP route. Both solid state reactions as well the liquid phase reactions were observed. It was reported that TSC prepared by HIP method had high bending strength and hardness than any other method [29]. Hot pressing methods limit the application area of sintered product. Pulse Discharge Sintering (PDS) technique was used for sintering of TSC. It is an innovative technique for rapid shrinkage, deducted from hot pressing sintering. In PDS computer aided control system is used, PDS requires less time compared to conventional sintering, the heating rate is too high; hence it can control grain coarsening. Sintering temperature was decreased by 100 - 200 °C for TSC by using PDS, it was reported to produce high density component at relatively lower temperatures and in shorter time [28]. It was reported that addition of small amount of Al in 3Ti/SiC/C system, sintering temperature of TSC was decreased. There are some reports on sintering of TSC by using pressure-less sintering. Pressure-less sintering of MAX phase powder is difficult, due to its easy decomposability at high temperatures, loss of Si from TSC or loss of Al from  $\text{Ti}_3\text{AlC}_2$  powders. Racault et al. [13] were the first to report the decomposition of  $\text{Ti}_3\text{SiC}_2$  into TiC and gaseous Si. They observed that decomposition occurred at 1450 °C using an alumina crucible, or at 1300 °C when using a graphite crucible. The same was confirmed by various authors. High density TSC product produced through pressureless sintering could be economical and also broadens application area. There are some reports on TSC production through pressureless sintering [1, 12]. They achieved sintering density around 96% without

sintering aid and 99% with sintering aid at 1 wt% of Si and 98% with sintering aid at 1wt% of Ni. TSC has a good combination of flexural strength, high temperature properties, oxidation resistance and corrosion resistance. The stress at fracture using the flexure test is known as flexural strength, this is an important mechanical property for brittle materials. In MAX phase for any microstructure flexural strength are typically 50% lower than the compressive strength [6]. Comparison of tensile, compressive and flexural strength for TSC has been shown in Table 2.1. MAX phase tested to undergo a brittle to plastic transition (BPT), It was reported that for TSC; BPT is in the range of 1150 °C to 1200 °C (Figure 2.2).

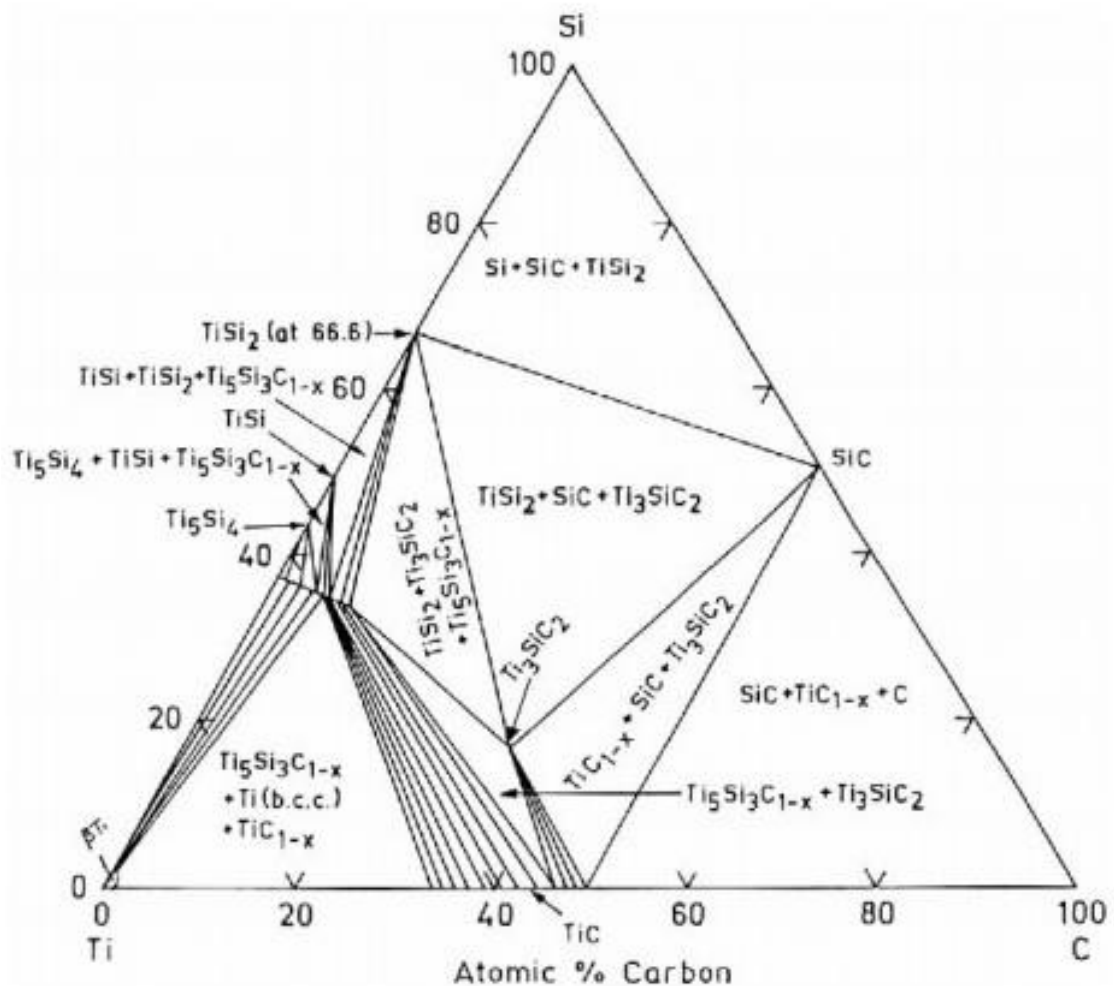


Figure 2.1: Isothermal sections of Ti-Si-C system at 1250 °C [36]

Table 2.1: Comparison of tensile, compressive and flexural strength with different microstructure of TSC [6]

Strength	Fine grain (Strength in MPa)	Coarse grain (Strength in MPa)
Tensile	298	180
Compressive	1050	720
Flexural	600	350

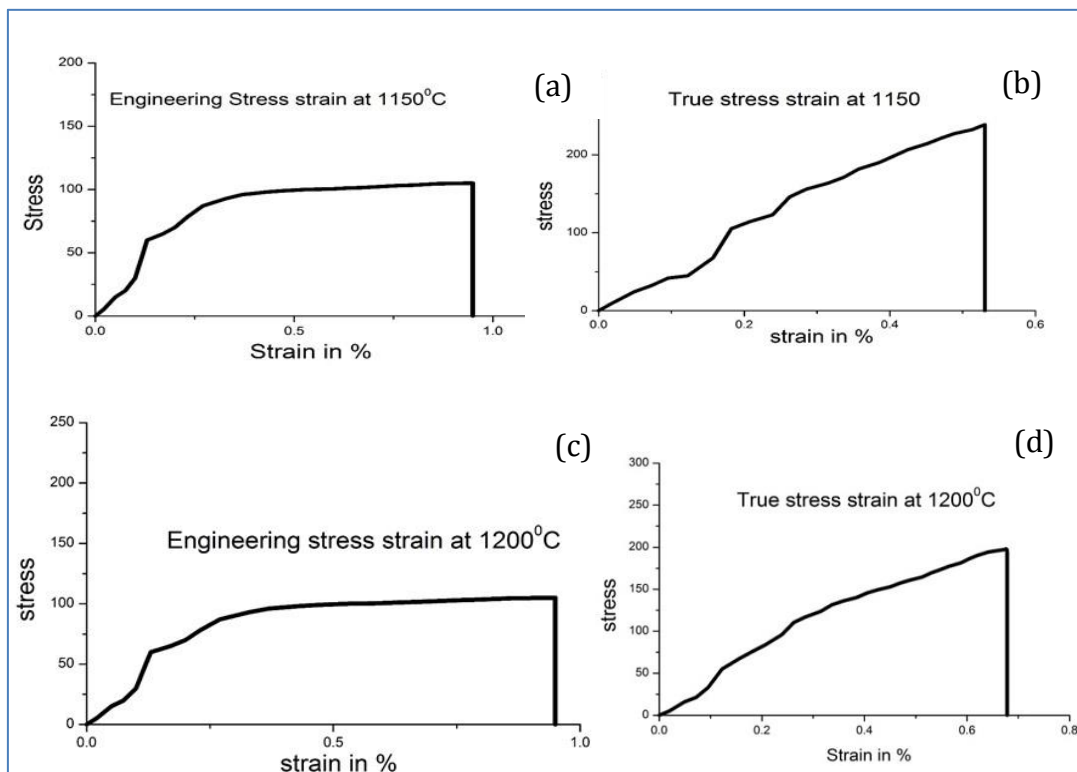


Figure 2.2: For Fine grain microstructure; Engineering stress Vs strain (a) & true stress Vs strain (b) at 1150 °C under tensile load are plotted. Engineering stress Vs strain (c) & true stress Vs strain (d) at 1200 °C under tensile load.

Reason behind plastic deformation at high temperature is Kink Band (KB) formation [2]. Response of TSC during compressive loading was reported by T. Zhen et. al [33] that at lower temperature the stress- strain curves are fully reversible whose size and shape depend on grain size but not on strain rate. Fine grain (size) and Coarse grain (size) microstructure becomes softer with increasing temperature; the initial slopes of the stress-strain cycles of both FG and CG materials were close to the true elastic

modulus of Fine grain samples, the response of the CG samples at 500 °C was comparable to that of the FG samples at 1100 °C, both the relaxation times and total recovered Strain was higher in the CG microstructure than FG (Figure 2.3). Tensile, relaxation and cycling loading–unloading tests indicated that the mechanical response of TSC has a strong dependence on temperature and strain rate, but a weak dependence on grain size [33]. At low temperature with high strain rate brittle failure was observed [34]. Thermal properties of TSC were reported by Barsoum et al. [35] that, amplitude of vibration of Si atoms was higher than Ti and C atoms. The amplitudes of vibration of the Ti atoms adjacent to the Si atoms were higher and more anisotropic than for the other Ti atom sandwiched between the C-layers. Thermal expansion coefficient was slightly different along the *a* and *c* axes.

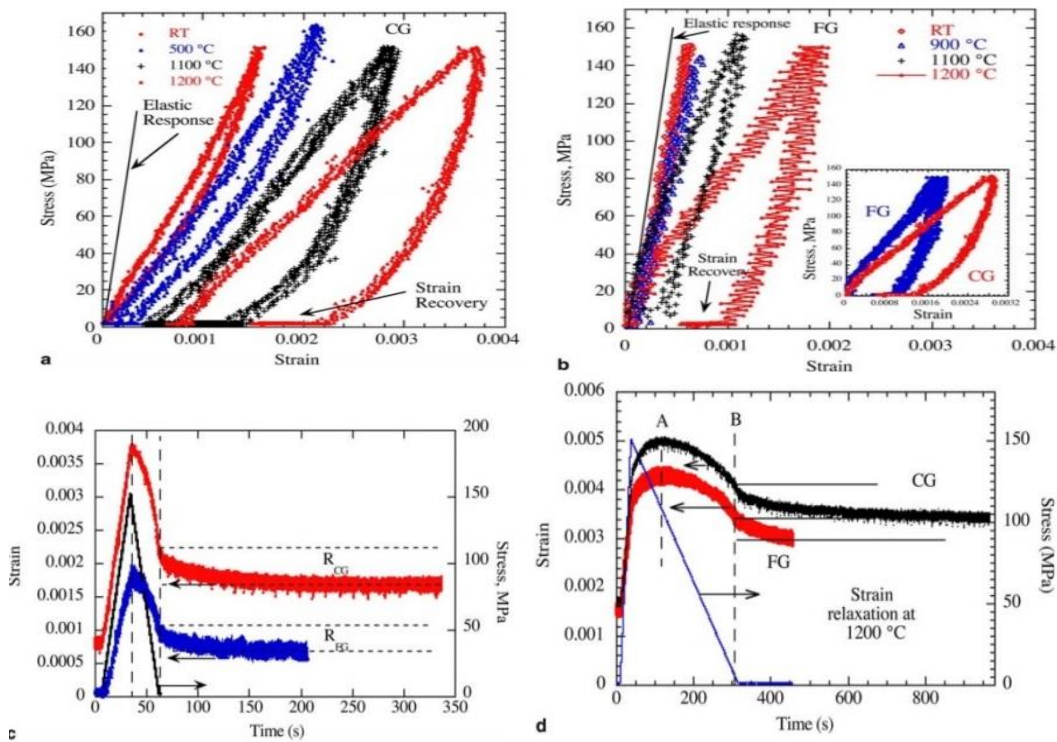


Figure 2.3: Temperature dependence of cyclic stress–strain for: (a) CG and (b) FG TSC samples. Inset in (b) compares the first cycles for both microstructures. Time dependencies of stress and strain during loading and unloading of both microstructures, for (c) relatively fast unloading, and (d) slower unloading respectively, at 1200 °C. Note time delay in the position of the maximum stress and maximum strain. Also note relaxation after load is removed [6].

The response to the thermal shock was reported to depend on the grain size. The coarse grained TSC was far better than the fine grained TSC. TSC is easily machinable & the holes are easily drillable with no lubrications. It was observed that TSC becomes self-lubricating during machining [4]. It was reported that TSC showed lower crack growth than the conventional ceramic during fatigue loading, the high fatigue resistance was originated from the heterogeneous and laminated structure. The creep behaviors of TSC were reported for tensile as well as compressive loadings; it was observed that the creep rates in compression were roughly an order of magnitude lower than that in tension [3].

Oxidation rate of TSC was found to be lower than the TiC. Oxidation in TSC occurs due to outward diffusion of Ti and carbon; and inward diffusion of oxygen. SiO<sub>2</sub> layer was found on TSC surface after short term oxidation at 1000 °C in air [3]. Corrosion resistance of TSC in acid or alkaline solutions was found to be better than pure Ti [3]. There are some applications of MAX phase materials like, rotating electrical contacts and bearings, heating elements, nozzles, heat exchangers, tools for die pressing. Self-lubrication property is advantageous over graphite in applications where rotating electrical contacts are required such as commutating brushes for AC motors. Many of these applications are currently being field tested and are at various stages of development. There are several hurdles to commercialization, including the relative high cost of the powders and sintered components compared with conventional ceramics such as SiC and alumina [1], etc.

It was reported that addition of sintering aids in TSC improves sintering density of TSC powder with small amount (1 and 2 wt. %) of Si powder, under pressureless condition. The final product had a very low amount of impurities [1]. There are no other reports on sintering kinetics of TSC powder in addition to the sintering aids. It has also been reported that nickel was used as sintering aid for the metal and ceramic powders, due to its ability to form intermetallic compound at high temperature as well as at low temperature. Nickel is known as fast diffuser in the metals like titanium and is found to enhance the sintering rates of titanium, tungsten and some ceramic powders. Addition of Ni in small amounts shows liquid phase sintering behavior. Bulk samples prepared



from TSC-1Ni, exhibited good mechanical properties. However, there are no reported studies on the sintering kinetic of TSC powder so far [9, 12]. A critical literature study shows that, still there are many issues, which need to be addressed, such as pressure-less sintering of TSC, effect of addition of sintering aids, microstructural changes due to sintering aids and effect of sintering aids on mechanical properties of TSC etc.

## **2.1 Objectives**

**The objectives of the present investigations are:**

- **To achieve high density parts through pressure-less sintering by adding sintering aids like Si, Ni and analyze effect of sintering aids.**
- **To study the sintering mechanism for isothermal heating by using Johnson's Model.**
- **To study sintering mechanism for non-isothermal heating by using Young & Cutler's Model.**

## Chapter 3

# Experimental Procedure

Titanium powder of 99.5 wt% purity (-325 mesh), graphite powder of 99 wt%, (7 to 11  $\mu\text{m}$ ) and Silicon powder of 99.5 wt% purity (-325 mesh) were procured from Alfa Aesar.

### 3.1 Synthesis

The experiments were conducted in three different stages: (i) Synthesis of  $\text{Ti}_3\text{SiC}_2$  powder, (ii) Pressureless sintering of  $\text{Ti}_3\text{SiC}_2$  and (iii) Dilatometry of  $\text{Ti}_3\text{SiC}_2$  with different sintering aids such as Nickel and Silicon. Synthesis of  $\text{Ti}_3\text{SiC}_2$  was carried out in two ways: (i) Synthesis of TiC and then synthesis of TSC; (ii) Direct synthesis by using elemental mixture of Ti, Si and graphite powders.

#### 3.1.1 Synthesis of $\text{Ti}_3\text{SiC}_2$ using $\text{TiC}_{0.67}+\text{Si}$

In first method, Ti and graphite powders are mixed in a molar ratio of 3:2 by agate mortar and pestle. Toluene was added for proper mixing. About 4% wt paraffin wax was added as a binder, for compaction. Powder was compacted uniaxially in a steel die (diameter of 10 mm) at low pressure ( $\sim$  20 MPa). These compacts were kept in alumina crucible and heated in a tubular furnace at 1300  $^{\circ}\text{C}$  for 90 minutes under flowing high purity argon gas, with heating rate of 10  $^{\circ}\text{C}/\text{min}$ . At 300  $^{\circ}\text{C}$ , 20 minutes hold was given for the evaporation of binder. Synthesized  $\text{TiC}_{0.67}$  was pulverized and sieved using -325 mesh size screens. The synthesized  $\text{TiC}_{0.67}$  powder was mixed with Si in a molar ratio of 3:1 by agate mortar and pestle. Samples were kept in tubular furnace up to 1200  $^{\circ}\text{C}$  in isothermal condition for 60 minutes under flowing high purity argon gas with heating rate of 10  $^{\circ}\text{C}/\text{min}$ .

#### 3.1.2. Synthesis of $\text{Ti}_3\text{SiC}_2$ through elemental powders

In second method elemental powders of Ti, Si and graphite were mixed in the molar ratio 3:1:2 by agate mortar and pestle. Toluene and 4 wt% paraffin wax was added.

Same procedure was followed for pellet preparation like  $\text{TiC}_{0.67}$  synthesis, as discussed in earlier section. Heating was carried out in tubular furnace made Inconel up to  $1100\text{ }^{\circ}\text{C}$  and kept at isothermal condition for 60 minutes, under flowing high purity Argon gas with heating rate of  $10\text{ }^{\circ}\text{C}/\text{min}$ . At  $300\text{ }^{\circ}\text{C}$  20 minutes hold was given for evaporation of binder. Synthesized Powder was pulverized and sieved using -325 mesh size screens. Since the degree of conversion to TSC was not very high, the product contain large amount of  $\text{TiC}_{0.67}$  and other impurities, therefore this synthesized product was further mixed in ball mill and reheated to  $1100\text{ }^{\circ}\text{C}$  for the isothermal condition of 60 minutes, to increase the conversion. This double heated powder pulverized and sieved using -325 mesh screens. For each experiment before synthesis Argon gas was flushed in tube for 30 minute to remove residual air. Powder which was synthesized by second method was used for sintering study.

## **3.2 Sintering**

Five types of powders were taken for sintering a) TSC powder b) mixed powders TSC + 1 wt% Si (designated as TSC-1Si), c) mixed powders TSC+ 2 wt% Si (designated as TSC-2Si), d) mixed powders TSC+ 1 wt% Ni (designated as TSC-1Ni) & e) mixed powders TSC+2 wt % Ni (designated as TSC-2Ni). About 4 wt% of paraffin wax as binder was first dissolved in toluene and then the powders were mixed (procedures were same for all types of powders). These powders mixed by agate mortar and pestle for about half an hour and dried while stirring continuously.

### **3.2.1 Sintering aids**

Small amount of additive causes large enhancement in sintering is called as activated sintering. Activated sintering is performed in the presence of small amounts of metal additives, at temperatures below the melting point of the additive, for solid state sintering. It is possible to lower the sintering temperature substantially through activated sintering.

### **3.2.2 Criteria for sintering aids**

It is important to analyses all phase diagrams of sintering aids with respect to all element which are present in parent material. The additives have to be insoluble in base

material at sintering temperature to inhibit grain growth. The mixture sits at a two phase region at the sintering temperature where melting points are depressed and the activator A is nearly insoluble in the base B, but the reverse solubility is required (Figure 3.1).

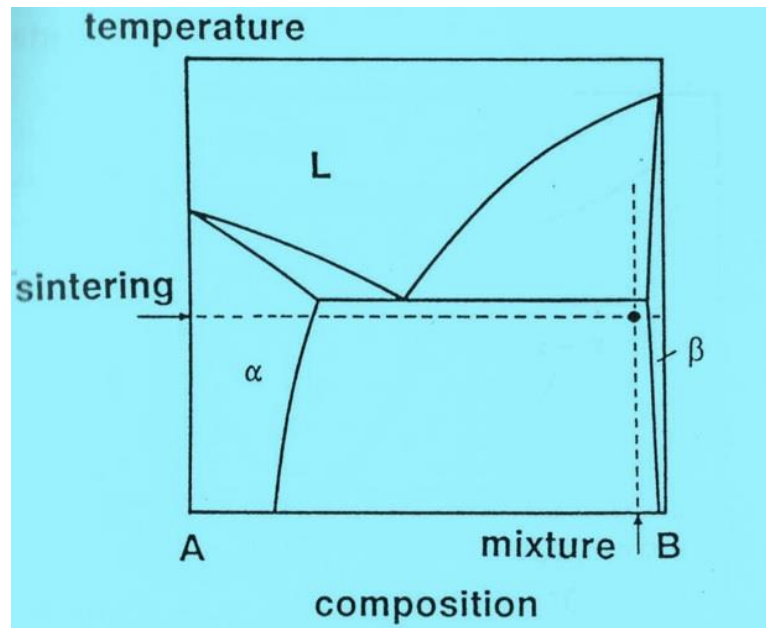


Figure 3.1: Idealized binary-phase diagram for solid-state activated sintering [25].

### 3.2.3 Selection of Ni and Si as sintering aids

Nickel is known as a fast diffuser in the metal and ceramic systems [24]. It is also observed that Ni suppressed grain coarsening process up to some extent during sintering [24]. It has been reported that for TSC, not only sintering density increase but also the mechanical properties [6]. Ni has good solubility in Ti as well as in Si at elevated temperature and forms many low melting intermetallic compounds. Therefore it is expected that Ni can act as sintering aid for TSC system. At high temperature sintering, there may be possibility of decomposition of TSC phase into TiC and loss of Si. Therefore additional Si is required to compensate the loss of Si and to increase the TSC formation while reacting with retained titanium carbides.

### 3.2.4 Pressureless Sintering

Powders were compacted uniaxially using steel die (7 mm diameter) at low pressure (20 MPa) and then cold isostatically pressed (CIP, Insmart Hyderabad, India) at a pressure of 200 MPa for a holding time of 1 min. The weight of each compact was around 0.5 gm. Green density of the cylindrical compact was estimated by their weight and dimensions. The green compacts were kept in alumina crucible and placed in to a tubular furnace. After loading the sample in furnace, high purity Argon gas was flushed in tube for half an hour, then furnace was heated at the rate of 10 °C/min. and held at 300 °C for 30 min. This step was carried out for removing binder (paraffin wax) completely. The furnace was heated up to 1500 °C for isothermal time of 60 min. The argon gas flow was continued till the end of cooling step. Cooling rate was 10 °C/min. Density measurements of sintered samples were carried out. The phase were determined using X-ray powder diffractometer (PANalytical X'Pert Pro) with Cu K $\alpha$  ( $\lambda = 1.5456$  Å, step size 0.01°) radiation. Micrographs were characterized by using scanning electron microscope (FESEM- CARLZEISS, SUPRA-40, Germany). Indentations were done on TSC and TSC-1Ni sintered samples using Vickers hardness test at 2 Kg load and 5 Kg load.

### 3.3 Dilatometry

Dilatometry has been used to study the sintering behavior of powder compacts. Dimensional change data is collected with respect to time and temperature. Dilatometer data was used for studying isothermal and non-isothermal behavior during sintering of TSC. For non-isothermal heating study, five types of powder were taken for Dilatometer experiment: a) TSC powder, b) TSC-1Si, c) TSC-2Si, d) TSC-1Ni and e) TSC-2Ni and similar methods (as prepared for pressureless sintering) were followed to prepare green compacts for dilatometer experiments. The green compact kept in sample holder (alumina), which was kept in dilatometer setup (Single push rod Dilatometer, Dilamatic II, Theta Industries US) with push rod carrying 25 gm of load. Experiment has been carried out for five different samples for non-isothermal heating upto 1500 °C. For isothermal heating study three green compacted samples of TSC were sintered in dilatometer at 1200 °C, at 1400 °C & at 1500 °C. Data were collected in the form of thermal expansion with respect to temperature and time.

### **3.4 Characterization**

Initially as received powders of titanium, silicon and graphite were characterized by using X-ray diffraction method. X-ray diffraction were done for  $\text{TiC}_{0.67}$  and TSC powders. Scanning electron microscope micrographs of synthesized powder of TSC were taken at different magnification, EDX were done for analyzing elemental composition (Working distance = 5 mm, EHT = 5 kV) for sintered samples were broken into two pieces. SEM micrographs of fractured surface were taken for all five samples at various magnifications. For X-ray characterization, samples were crushed and formed powder by using agate mortar and pestle followed by sieving by using -325 mesh size. Dimensional and weight measurement of the green compact and sintered samples were carried out. Experimental procedure has been outlined by flow chart (Figure 3.1).

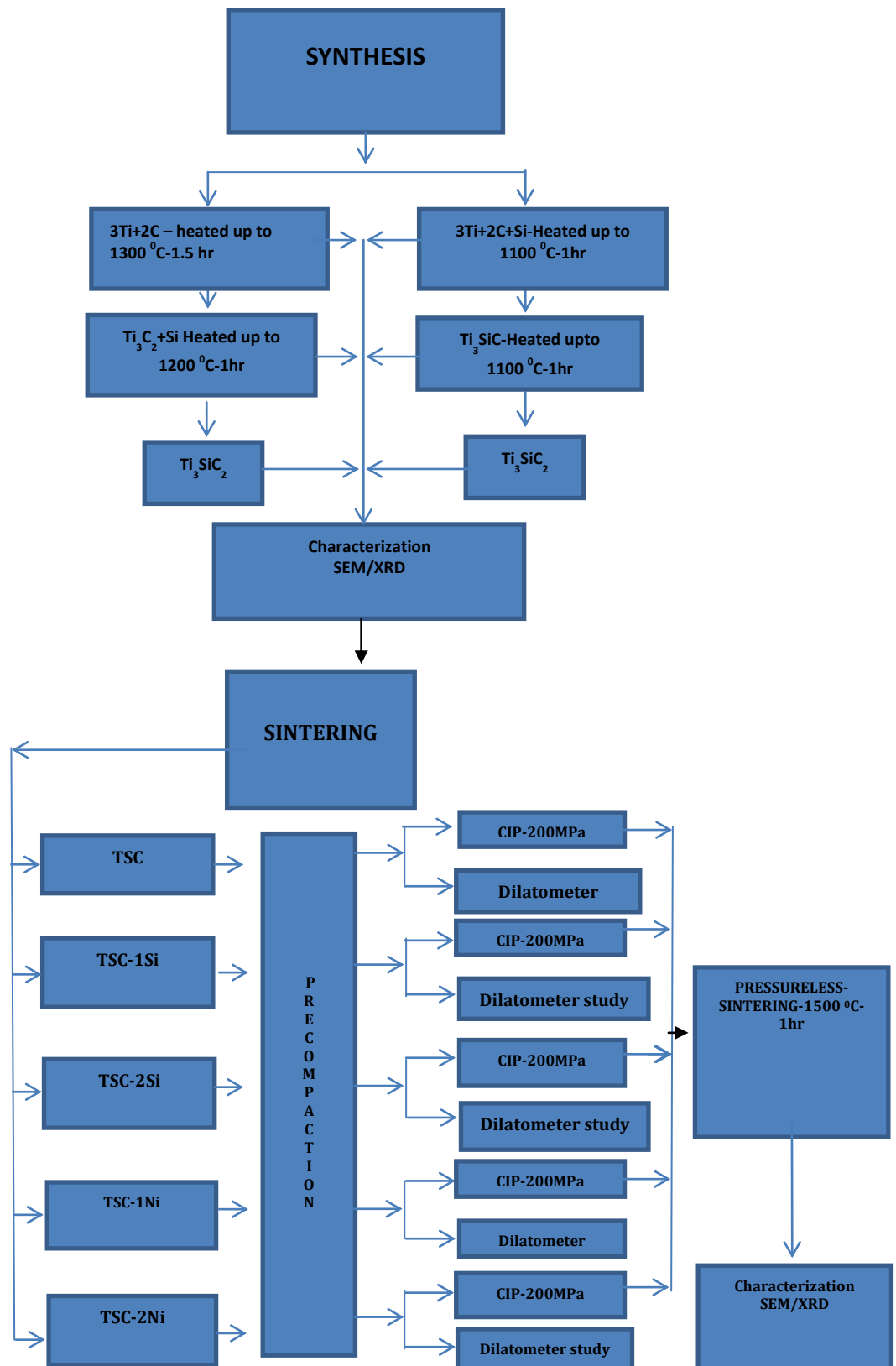


Figure 3.1: Flow chart of experimental procedure

## Chapter 4

# Results and Discussion

Figure 4.1 represents the XRD pattern of as received Ti, Si and graphite powders. It has been compared with their standard JCPDS (Ti-441294, Si-271402, and Graphite-411487) data for phase identification.

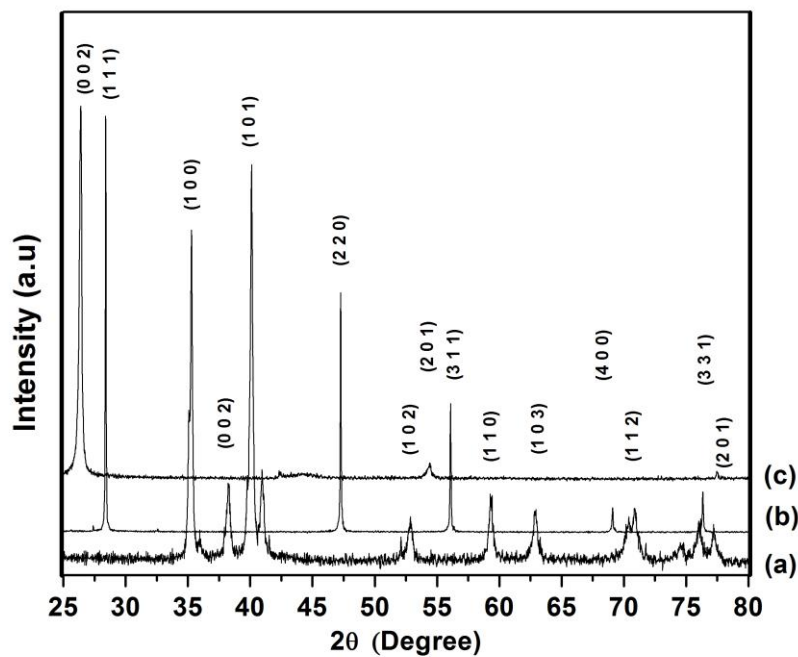


Figure 4.1: XRD- pattern of as- received powders: a) pure Ti, b) pure Si & c) pure graphite

### 4.1 Synthesis

XRD-pattern of TSC synthesized by two stage method has been shown in Figure 4.2. XRD graph were compared with their standard JCPDS (TiC- 652224, TSC-653559,  $\text{TiSi}_2$ -710187) data for phase identification. It appears that TiC did not react well with Si. Major peaks belong to TiC phase, where as TSC and  $\text{TiSi}_2$  were present in small fractions. XRD- pattern of synthesized TSC by elemental powders has been shown in Figure 4.3. Major peaks belong to TSC and other phases like TiC and TiSi are



reminder. It has been observed from XRD (Figure 4.3); after double heating some peaks were disappeared. XRD pattern of synthesized powder by first method showed that, TSC phase was present in small fraction, while TiC phase was the major fraction. The reason for these results could be due to problem with received titanium powder as it was slightly oxidized on surface and also some amount of silicon loss was observed.

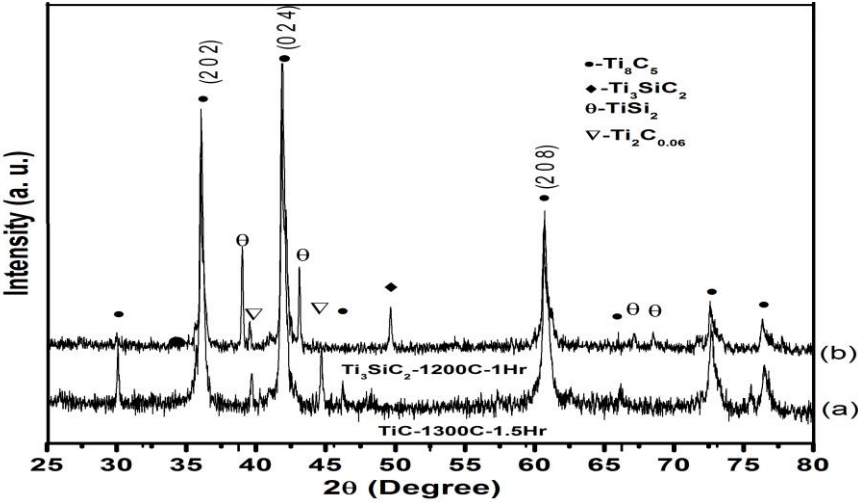


Figure 4.2: XRD pattern of TiC-synthesized at 1300 °C-1.5 hr. and TSC synthesized at 1200 °C-1 hr.

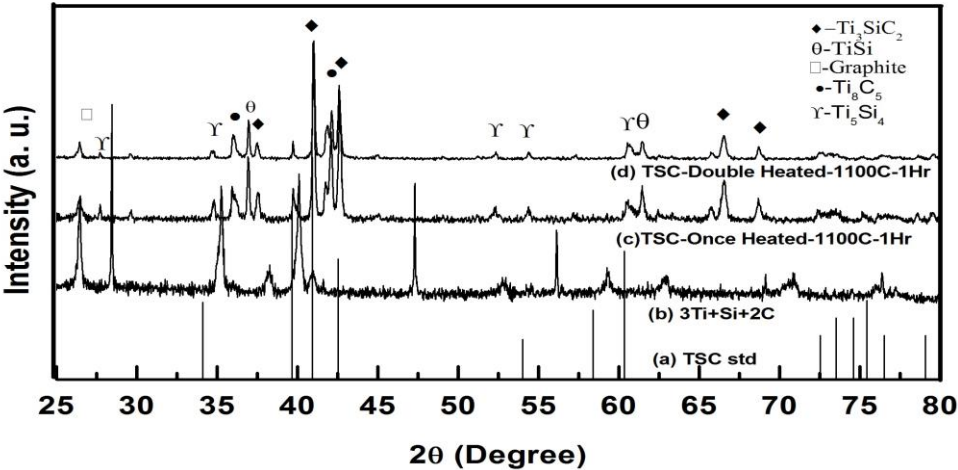


Figure 4.3: X-ray diffraction pattern of, a) TSC JCPDS b) mixed 3Ti+Si+2C powder, c) once heated TSC at 1100 °C- 1 hr & d) double heated TSC at 1100 °C- 1 hr.

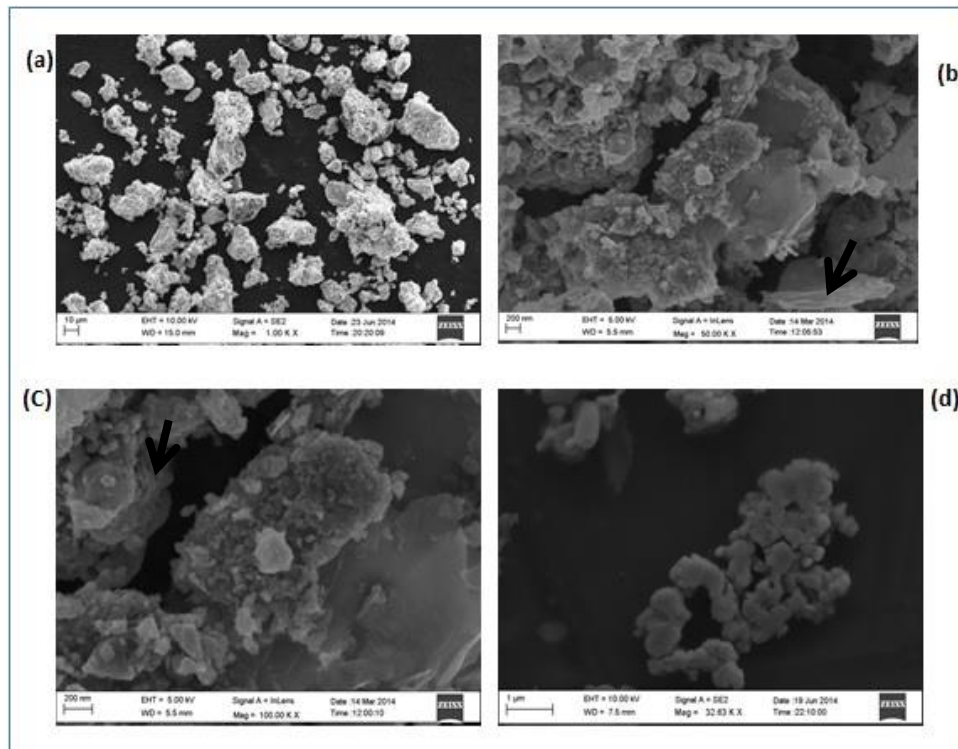


Figure 4.4: SEM micrograph of synthesized powder at 1100 °C-60 minutes (double heated): a) at 1 KX, b) at 50 KX (stepped surface particles are shown by arrow), c) at 100 KX (stepped surface particles are shown by arrow) and d) agglomerated particles at 30 KX

In the second method, it was observed that synthesis of TSC was possible through elemental powder synthesis route, synthesized TSC had particle size ranging from 4 µm to 40 µm and some particles were agglomerated [Figure 4.4 (a)]. Stepped surface particles are observed [shown by arrow in Figure 4.4 (b)], white color particles are titanium carbides [Figure 4.4 (c)], agglomerated particles are shown at high magnification- 32KX [Figure 4.4 (d)].

## 4.2 Sintering

Figure 4.5 represents XRD pattern of all five samples sintered at 1500 °C. It was observed from XRD pattern (Figure 4.5) that TSC phase was decomposed from all samples (TSC, TSC-1Si, TSC-2Si, TSC-1Ni & TSC-2Ni). Decomposition of TSC phase leads to form TiC phase. At 1500 °C all samples decomposed and form TiC as

major phase. SEM micrograph of fractured surface of sintered samples indicates, few particles have stepped surface that represents presence of TSC phase. EDX analysis of sintered samples confirms elemental presence on all powders. Sintering additives have played role in on-set sintering temperature and shrinkage behavior during sintering.

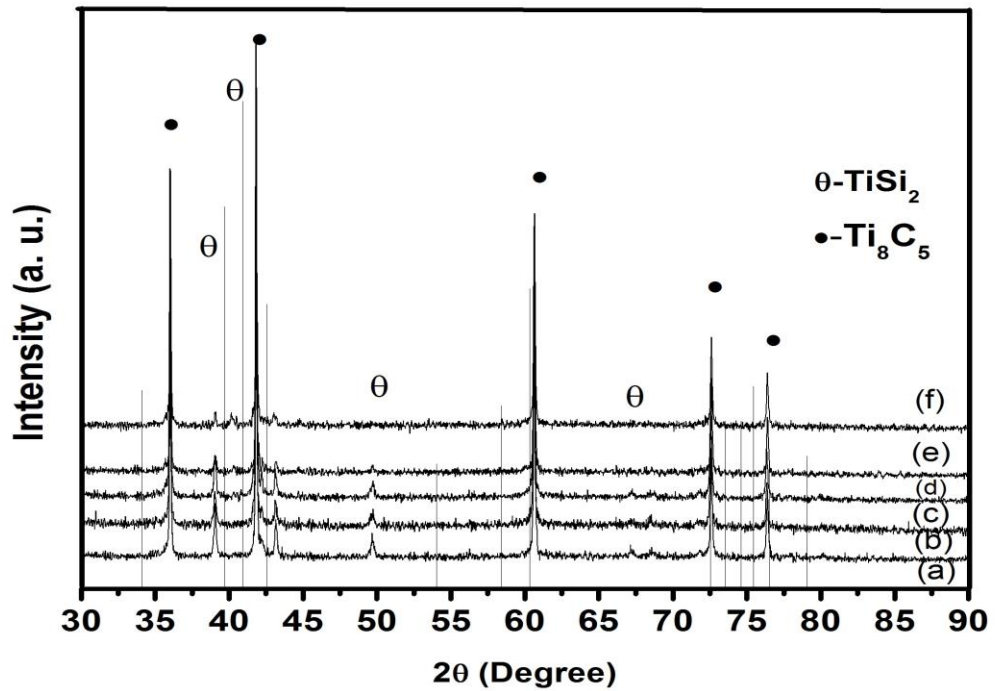


Figure 4.5: XRD pattern of pressureless sintered samples b) TSC, c) TSC-1Si, d) TSC-2Si, e) TSC-1Ni and f) TSC-2Ni at 1500 °C.

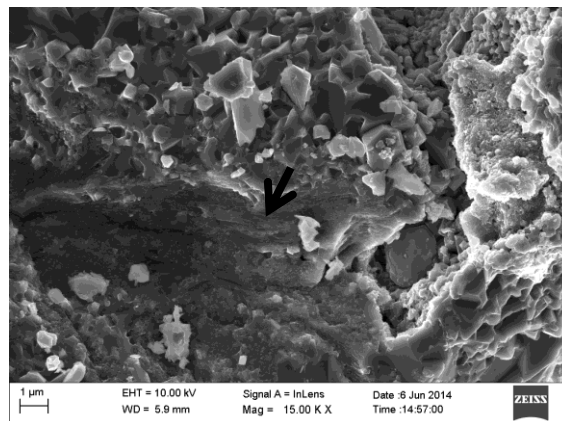


Figure 4.6: SEM micrograph of fracture surface of Sintered TSC sample at 1500 °C, ductile fracture shown by arrow.

It has been observed that particles are in irregular shape, some fractured particles are showing stepped surface, at some places ductile fracture was observed (Figure 4.6). Figure 4.7: represents EDX analysis of fractured surface of TSC sample sintered at 1500 °C-1 hr. and elemental mapping for Ti & Si [Figure 4.7 (b)]. It was observed that distribution of Ti was in proportion [Figure 4.7 (c)], Si was not dispersed well, and Si rich regions were formed [Figure 4.8 (d)]. Figure 4.8 represents SEM micrograph of fractured surface of sintered samples at 1500 °C-60 minutes isothermally hold, it was observed that samples are not dense, in TSC-1Si few particles are showing stepped surface shown by arrow [Figure 4.8 (a)]. In TSC-2Si plate like particles are observed in SEM micrograph indicating preferential growth of MAX phase grains [Figure 4.8 (b)], in TSC-1Ni and in TSC-2Ni at some places fractured surfaces show ductile failure [Figure 4.8 (c) & (d)]. Figures 4.9, 4.10, 4.11, and 4.12 show EDX analysis of TSC-1Si, TSC-2Si, TSC-1Ni and TSC-2Ni samples respectively. It was observed that Si and Ti are well dispersed in TSC-1Si [Figure 4.9 (c) & (d)]. In TSC-2Si distribution of Ti was in proportion [Figure 4.10 (C)], content of Si was increased [Figure 4.10 (d)] and it was well distributed. [Figure 4.11(b), (c) & (d)] & [Figures 4.12(b), (c) & (d)] show distribution in proportion for Ni, Ti & Si elements respectively.

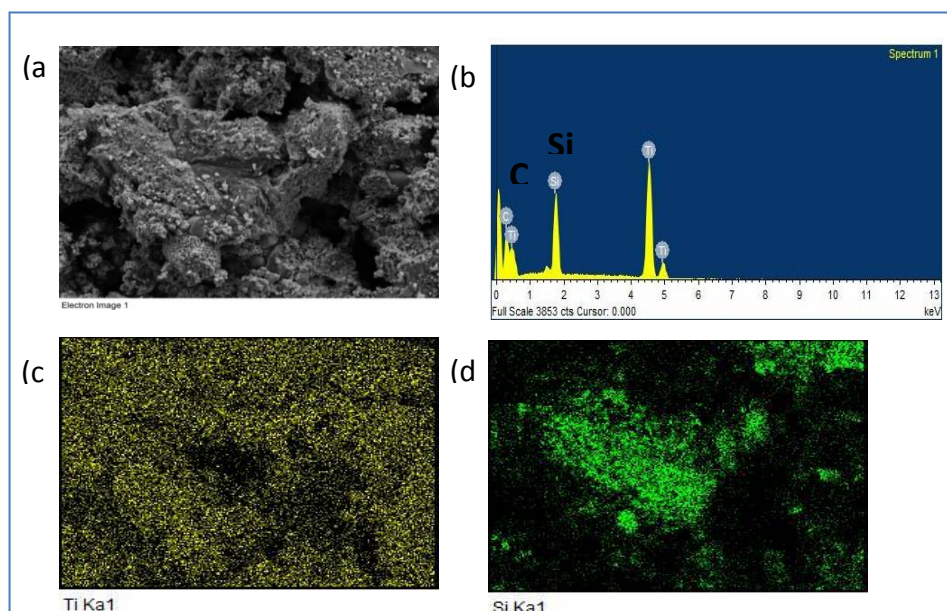


Figure 4.7: EDX analysis of Sintered sample-TSC-1500 °C-1 hr a) SEM micrograph considered for EDX, b) graphical representation of elemental mapping c) distribution of Ti d) distribution of Si.

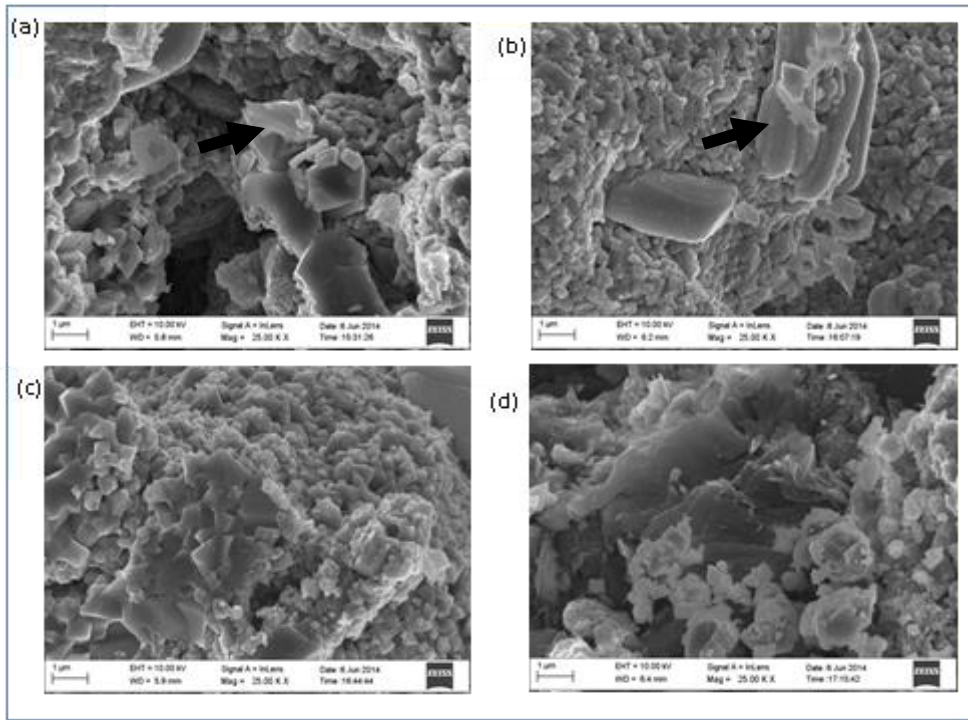


Figure 4.8: SEM micrograph fractured surface of sintered samples at 1500 °C-1 hr.  
 a) TSC-1Si, b) TSC-2Si, c) TSC-1Ni & d) TSC-2Ni

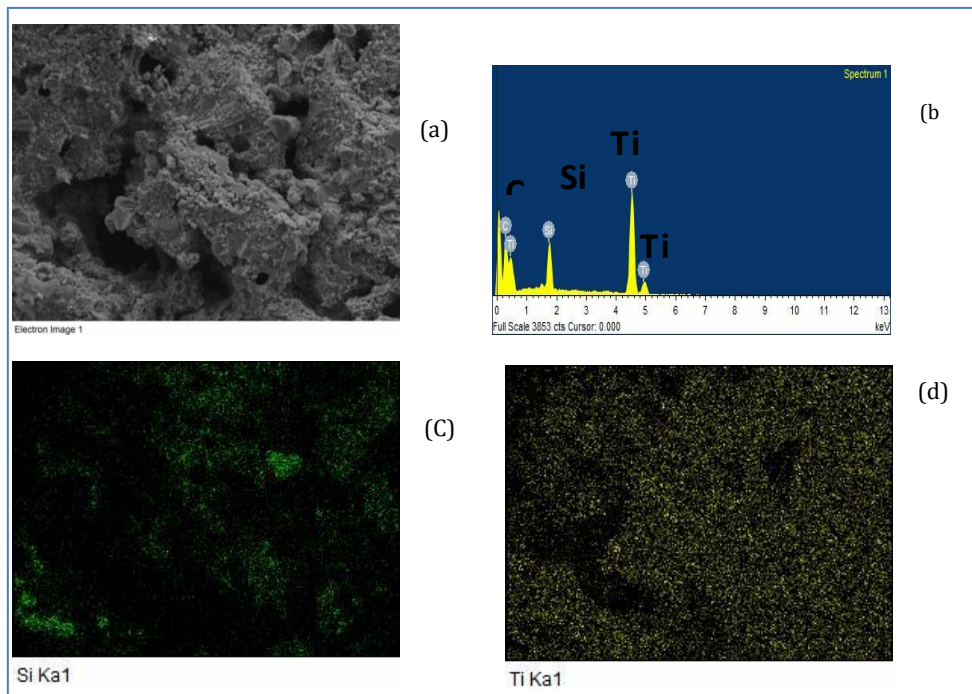


Figure 4.9: EDX of Sintered sample TSC-1Si-1500 °C: a) SEM micrograph considered for EDX, b) graphical representation of elemental mapping c) distribution of Ti d) distribution of Si

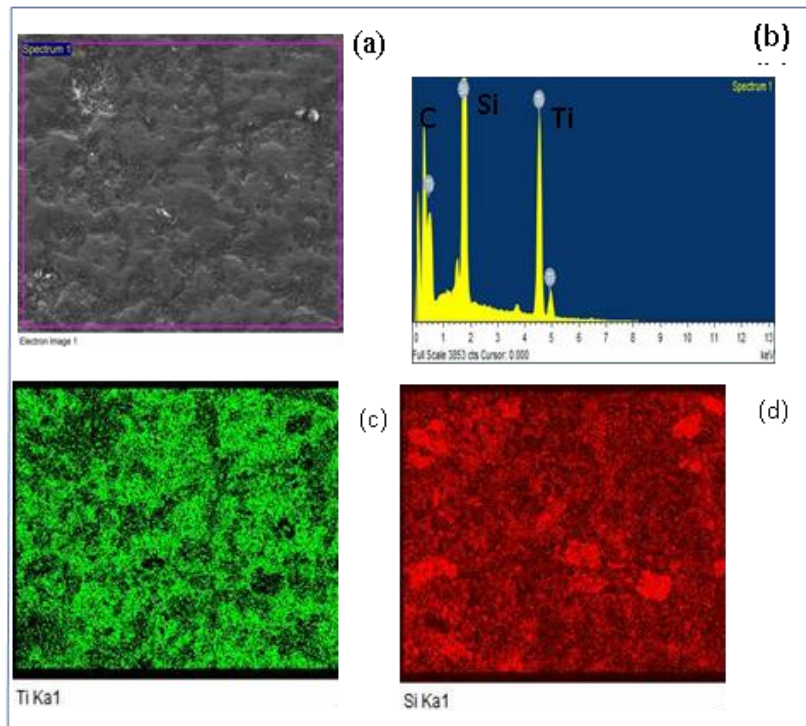


Figure 4.10: EDX analysis of sintered samples TSC-1Si-1500 °C: a) SEM micrograph considered for EDX, b) graphical representation of elemental mapping, c) distribution of Ti & d) distribution of Si

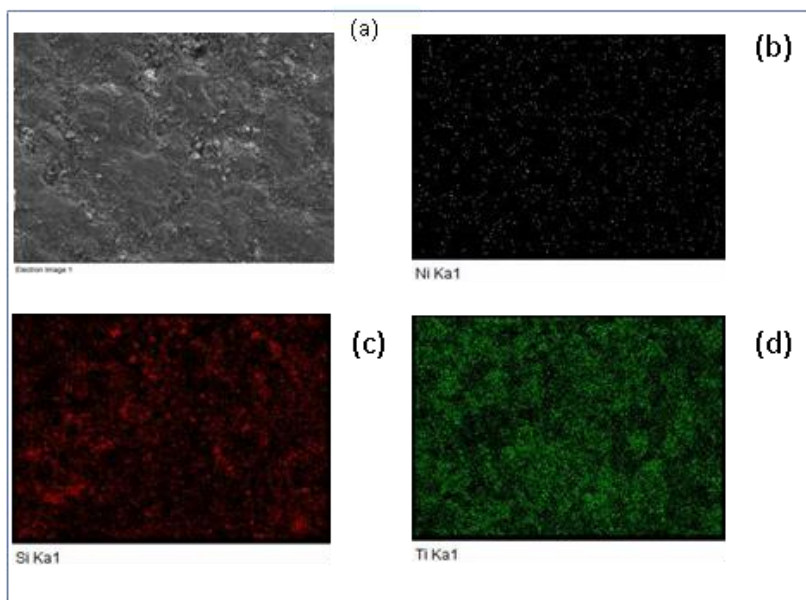


Figure 4.11: EDX of Sintered sample-1Ni-TSC-1500 °C a) SEM micrograph considered for EDX, b) Distribution of Ni, c) Distribution of Si & d) Distribution of Ti

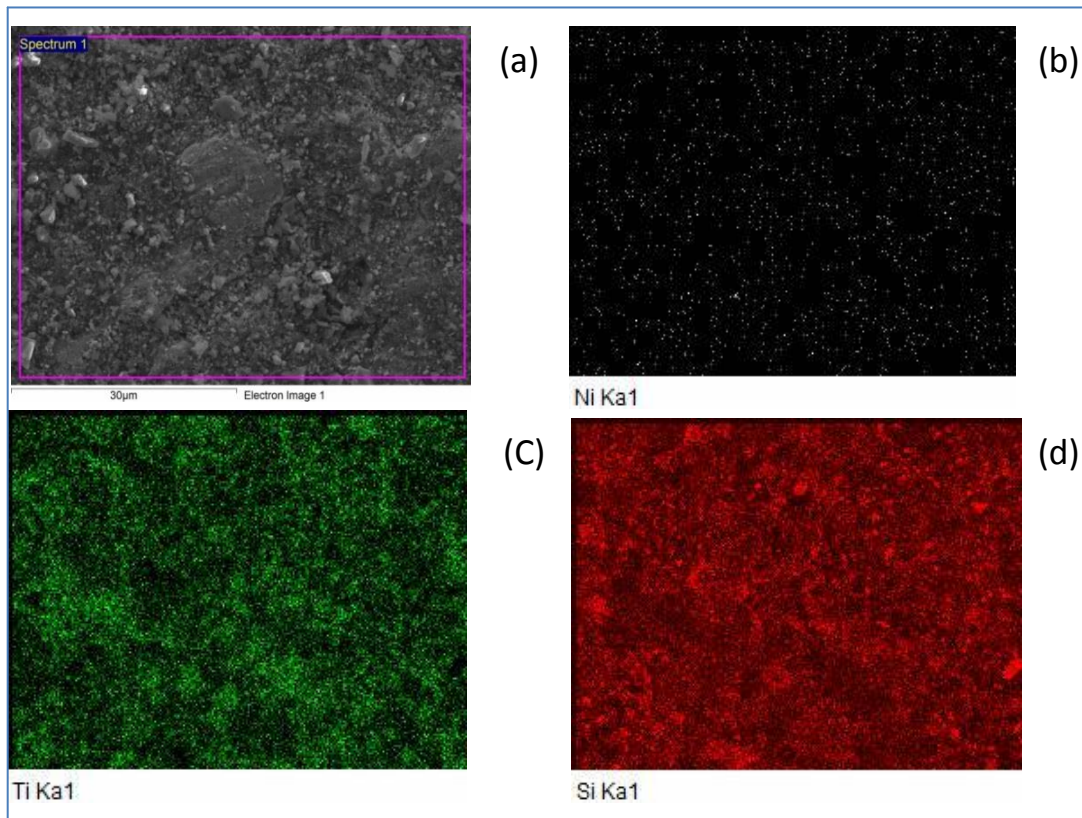


Figure 4.12: EDX of fractured surface of sintered samples of TSC-2Ni 1500 °C a) SEM micrograph considered for EDX, b) Distribution of Ni, c) Distribution of Ti & d) Distribution of Si

Density of sintered samples and green density have been represented in Table 4.1; all sintered samples are having relative density in the range of 60 to 75 % (theoretical density of TSC-4.5 gm/cm<sup>3</sup> has been taken for reference).

Table 4.1 Density of Samples with respect to theoretical density of Ti<sub>3</sub>SiC<sub>2</sub> Sintered at 1500 °C

SAMPLE	Green density in %	Sintered density %
TSC	59	67
TSC-1Si	55	60
TSC-2Si	54	70
TSC-1Ni	55	75
TSC-2Ni	53	60

### 4.3 Dilatometry

Dilatometer plot for TSC has been shown in Figure 4.13. It was observed that on-set sintering temperature was around 900 °C during isothermal holding at 1500 °C samples shows rapid shrinkage.

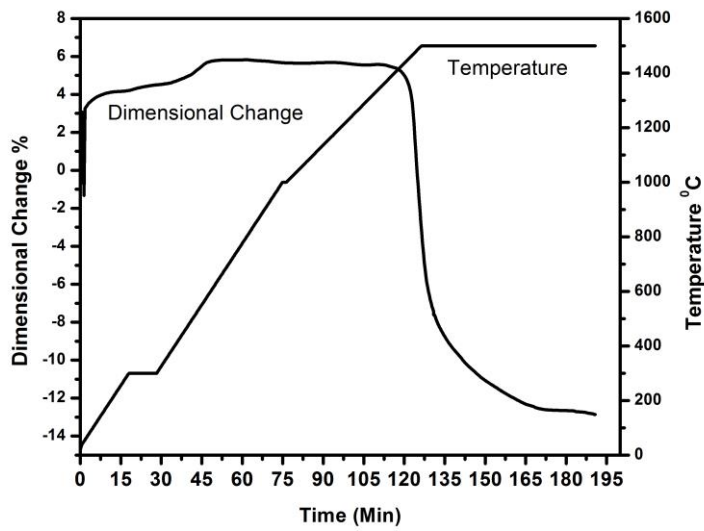


Figure 4.13: Dilatometer plot of TSC sintered at -1500°C for 1-hr

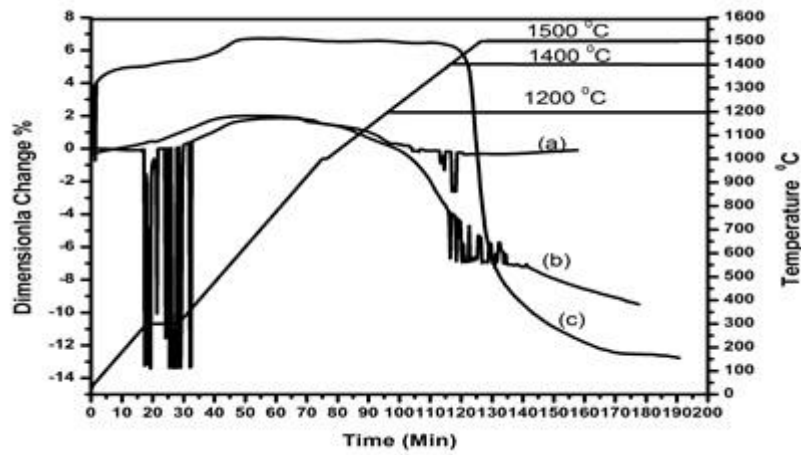


Figure 4.14: Dilatometer plots for TSC sample sintered at: a) 1200 °C, b) 1400 °C & c) 1500 °C



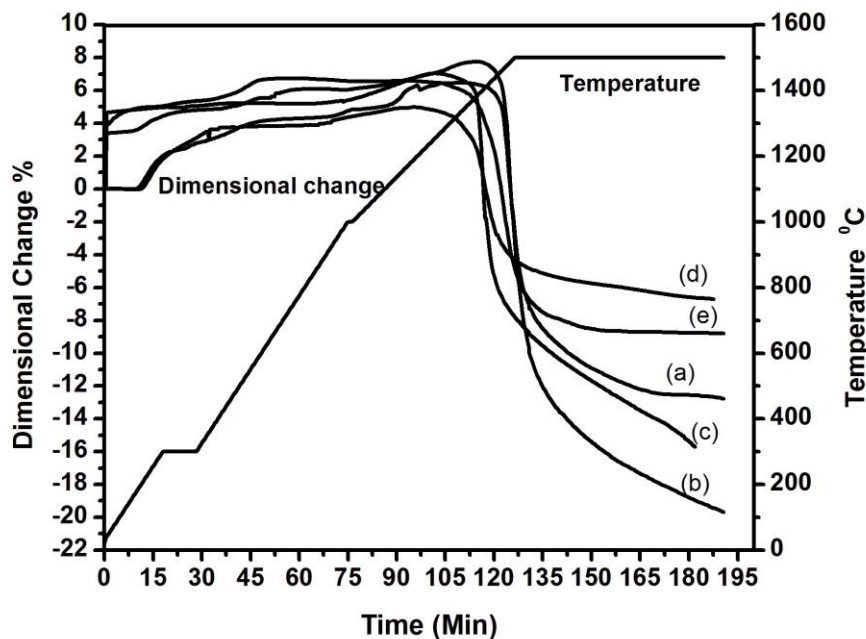


Figure 4.15: Dilatometer plots for: a) TSC, b) TSC-1Si, c) TSC-2Si, d) TSC-1Ni & e) TSC-2Ni sintered at 1500 °C

Figure 4.14 shows Dilatometer plots for TSC samples sintered at various temperatures. Very less shrinkage was observed in TSC-1200 °C (Figure 4.14 a), about 9% shrinkage was observed in TSC-1400 °C (Figure 4.14 b), rapid shrinkage was observed for TSC-1500 °C during isothermal holding (Figure 4.14 c). Figure 4.15 shows dilatometer plots for TSC, TSC-1Si, TSC-2Si, and TSC-1Ni & TSC-2Ni. It was observed that on-set sintering temperature for TSC-1Si was 1300 °C (Figure 4.15 b), on-set sintering temperature for TSC-2Si was 1400 °C (Figure 4.15 c) & on-set sintering temperature for TSC-1Ni was 1280 °C (Figure 4.15 d) and on-set sintering temperature for TSC-2Ni was 1230 °C (Figure 4.15 e).

#### 4.3.1 Analysis of isothermal sintering

Dilatometer data has been analyzed for TSC- samples which were heated up to 1200 °C, 1400 °C & 1500 °C and isothermally hold for 60 minutes. Dimensional change data has been collected from the time where isothermal holding starts to the time where it

ends. Reference line is theoretical thermal expansion line for TSC. Shrinkage ( $S_n$ ) measured from reference line to thermal expansion curves for TSC-1200 °C, TSC-1400 °C & TSC-1500 °C has been shown in Figure 4.16, 4.17 & 4.18 respectively.

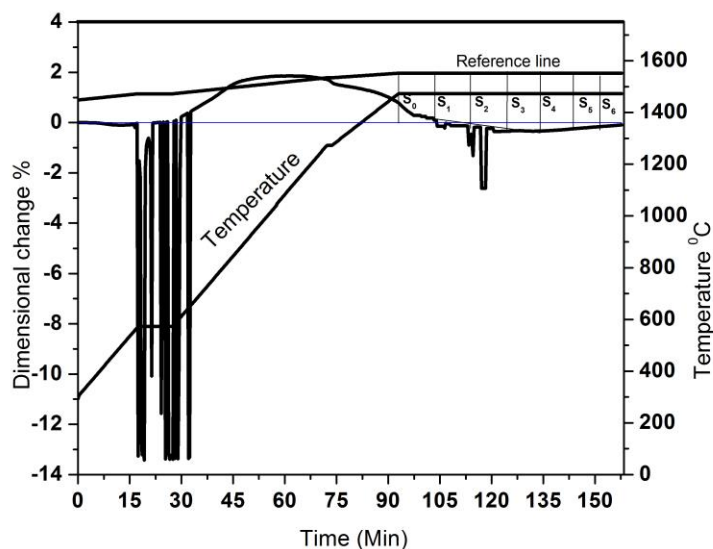


Figure 4.16: Measurement of shrinkage from dilatometer plot of TSC-1200 °C;  $S_0$ ,  $S_1$ ,  $S_2$  etc. are shrinkages at different times.

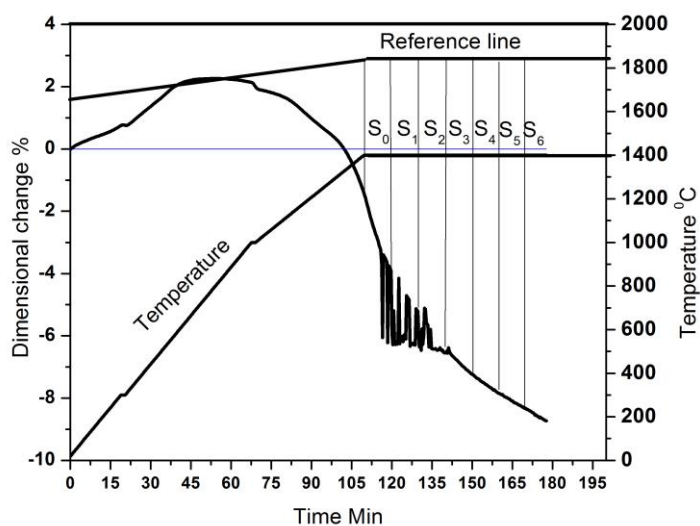


Figure 4.17: Measurement of shrinkage from dilatometer plot of TSC-1400 °C,  $S_0$ ,  $S_1$ ,  $S_2$  etc. are shrinkages

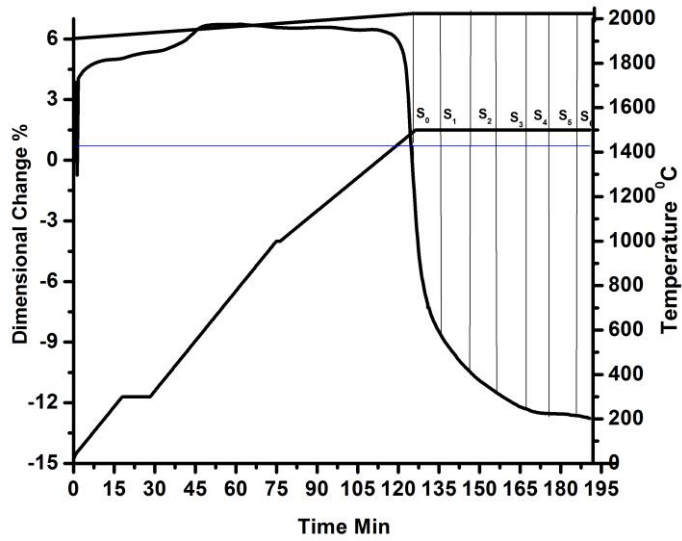


Figure 4.18: Measurement of shrinkage from dilatometer plot of TSC-1500 °C,  $S_0$ ,  $S_1$ ,  $S_2$  etc. are shrinkages.

Shrinkage and shrinkage rate were calculated for 1200 °C, 1400 °C & 1500 °C by using equation

$$\text{Shrinkage (Y)} = S_n / L_1$$

Where  $S_n = S_0, S_1, S_2, S_3, S_4, S_5$ .

$$L_1 = L_0 + h,$$

$h$  = Distance between reference line where isothermal hold starts to base line in mm

$L_0$  = Initial length of sample in mm.

$$\text{Shrinkage rate (Y}^*) = Y_n / t_n \tag{1}$$

$t$  = time in seconds,  $t_0 = 0$ ,  $t_1 = 10 * 60$ ,  $t_2 = 20 * 60$ , , ,  $t_n$ .

For TSC, Shrinkage was found to increase with increasing sintering temperature (Figure 4.19). It was observed that, for TSC-1500 °C & for TSC-1400 °C shrinkage rates were decreased with increasing time [Figure 4.20 (c) & (b)], for TSC-1200 °C shrinkage rate was slow. Johnson's sintering models [36] were used for estimation of grain boundary diffusion coefficient and volume diffusion coefficient and activation energies; as shown in equation (2) & (3).

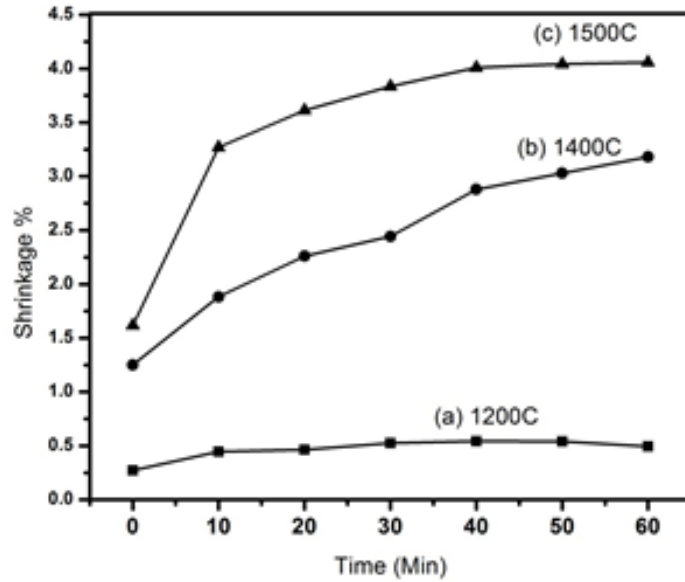


Figure 4.19: Measured shrinkage as function of isothermal holding time for TSC sintered at temperatures a) 1200 °C, b) 1400 °C & c) 1500 °C

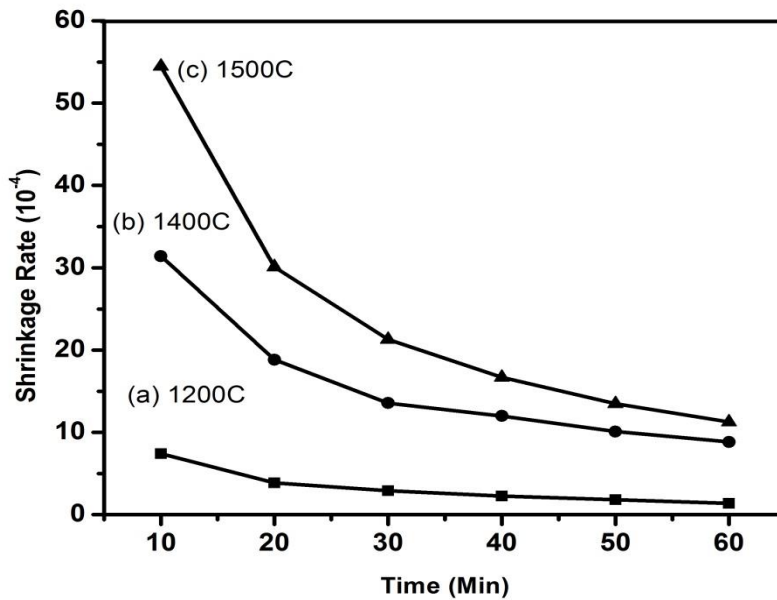


Figure 4.20: Shrinkage rate as function of isothermal time plot for TSC samples sintered at: a) 1200 °C, b) 1400 °C & c) 1500 °C

For grain boundary diffusion

$$\left( Y^{2.03} \frac{dY}{dt} \right) = \left\{ \frac{(2.14 \Omega \gamma b D_b)}{(kTr^4)} \right\} \quad (2)$$

For volume diffusion

$$\left( Y^{1.04} \frac{dY}{dt} \right) = \left\{ \frac{(5.34 \gamma \Omega D_v)}{(kTr^3)} \right\} \quad (3)$$

Where,

t = time in seconds,

$\gamma$  = surface free energy of TSC =  $55.4 \times 10^{-3} \text{ J/m}^2$ ,

T = temperature in degree Kelvin,

K = Boltzmann constant =  $1.38064 \times 10^{-23} \text{ m}^2 \text{ kg s}^{-2} \text{ K}^{-1}$ ,

$D_b$  = Coefficient of grain boundary diffusion,

B = Grain boundary width,

$\Omega$  = Atomic volume of TSC =  $7.18 \times 10^{-29} \text{ m}^3$ ,

$D_v$  = Coefficient of volume diffusion,

r = radius of particle (m)

Calculations of  $\ln(bD_b)$  &  $\ln(D_v)$  at 1200 °C, 1400 °C & 1500 °C for isothermal time 30 min and 60 minute are tabulated in tables 4.2, 4.3, 4.4, 4.5, 4.6 & 4.7. Logarithmic plots of the  $\ln(bD_b)$  and  $\ln(D_v)$  with respect to the inverse of temperature were plotted for estimation of activation energy and frequency factor for particle size of 8  $\mu\text{m}$ , 24  $\mu\text{m}$  and 32  $\mu\text{m}$  (Figure 4.21). To determine the activation energy for the any particle size equation (4) was used. Activation energy and frequency factor were calculated at time 30 min & 60 min (Table 4.5 & 4.6). It was observed that as particle size increases activation energy decreases. There was not a significant change in activation energy as time increases from 30 min to 60 min.

$$\ln(bD_b) = \left\{ \ln(D_0) - \left( \frac{Q}{RT} \right) \right\} \quad (4)$$

Where, R = 8.314 Joule/mole,

T = temperature (K)

Table 4.2: Calculations of  $\ln(bD_b)$  values for 8  $\mu\text{m}$  size particle, For TSC samples sintered at 1200  $^{\circ}\text{C}$ , 1400  $^{\circ}\text{C}$  & 1500  $^{\circ}\text{C}$  for the isothermal time of 30 min & 60 min.

Temp. ( $^{\circ}\text{C}$ )	$bD_b$ $t=30\text{min}$ ( $\text{m}^3/\text{s}$ )	$\ln(bD_b)$ $t=30\text{ min}$	$bD_b$ $t=60\text{min}$ ( $\text{m}^3/\text{s}$ )	$\ln(bD_b)$ $t=60\text{ min}$
1200	$4.2 \times 10^{-24}$	-53.8	$3.1 \times 10^{-24}$	-54.1
1400	$3.3 \times 10^{-21}$	-47.1	$3.2 \times 10^{-21}$	-47.2
1500	$1.3 \times 10^{-20}$	-45.7	$8.2 \times 10^{-21}$	-46.2

Table 4.3: Calculations of  $\ln(bD_b)$  values for 24  $\mu\text{m}$  size particle, For TSC samples sintered at 1200  $^{\circ}\text{C}$ , 1400  $^{\circ}\text{C}$  & 1500  $^{\circ}\text{C}$  for the isothermal time 30 min & 60 min.

Temp. ( $^{\circ}\text{C}$ )	$bD_b$ $t=30\text{min}$ ( $\text{m}^3/\text{s}$ )	$\ln(bD_b)$ $t=30\text{ min}$	$bD_b$ $t=60\text{min}$ ( $\text{m}^3/\text{s}$ )	$\ln(bD_b)$ $t=60\text{ min}$
1200	$3.4 \times 10^{-22}$	-49.4	$2.5 \times 10^{-22}$	-49.7
1400	$2.6 \times 10^{-19}$	-42.7	$2.6 \times 10^{-19}$	-42.8
1500	$1.1 \times 10^{-18}$	-41.3	$6.6 \times 10^{-19}$	-41.8

Table 4.4: Calculations of  $\ln(bD_b)$  values for 32  $\mu\text{m}$  size particle, For the TSC samples sintered at 1200  $^{\circ}\text{C}$ , 1400  $^{\circ}\text{C}$  & 1500  $^{\circ}\text{C}$  for the isothermal time 30 min & 60 min.

Temp. ( $^{\circ}\text{C}$ )	$bD_b$ $t=30\text{min}$ ( $\text{m}^3/\text{s}$ )	$\ln(bD_b)$ $t=30\text{ min}$	$bD_b$ $t=60\text{min}$ ( $\text{m}^3/\text{s}$ )	$\ln(bD_b)$ $t=60\text{ min}$
1200	$4.5 \times 10^{-21}$	-46.8	$3.3 \times 10^{-21}$	-47.1
1400	$8.5 \times 10^{-19}$	-41.6	$8.2 \times 10^{-19}$	-41.6
1500	$3.4 \times 10^{-18}$	-40.2	$2.1 \times 10^{-18}$	-40.7

Table 4.5: Calculations of  $\ln(D_v)$  values for 8  $\mu\text{m}$  size particle for the TSC samples sintered at, 1200  $^{\circ}\text{C}$ , 1400  $^{\circ}\text{C}$  & 1500  $^{\circ}\text{C}$  for the isothermal time 30 min & 60 min.

Temp. ( $^{\circ}\text{C}$ )	$D_{v\ t=30\text{min}}$ ( $\text{m}^2/\text{s}$ )	$\ln(D_{v\ t=30\text{min}})$	$D_{v\ t=60\text{min}}$ ( $\text{m}^2/\text{s}$ )	$\ln(D_{v\ t=60\text{min}})$
1200	$7.5*10^{-17}$	-37.1	$5.6*10^{-17}$	-37.4
1400	$1.3*10^{-14}$	-32.1	$1.1*10^{-14}$	-32.2
1500	$3.4*10^{-14}$	-31.1	$1.9*10^{-14}$	-31.5

Table 4.6: Calculations of  $\ln(D_v)$  values for 24  $\mu\text{m}$  size particle for TSC samples sintered at, 1200  $^{\circ}\text{C}$ , 1400  $^{\circ}\text{C}$  & 1500  $^{\circ}\text{C}$  for the isothermal time 30 min & 60 min.

Temp. ( $^{\circ}\text{C}$ )	$D_{v\ t=30\text{min}}$ ( $\text{m}^2/\text{s}$ )	$\ln(D_{v\ t=30\text{min}})$	$D_{v\ t=60\text{min}}$ ( $\text{m}^2/\text{s}$ )	$\ln(D_{v\ t=60\text{min}})$
1200	$2.1*10^{-15}$	-33.8	$1.5*10^{-15}$	-34.1
1400	$3.4*10^{-13}$	-28.7	$2.7*10^{-13}$	-28.9
1500	$9.1*10^{-13}$	-27.7	$5.3*10^{-13}$	-28.2

Table 4.7: Calculations of  $\ln(D_v)$  values for 32 $\mu\text{m}$  size particle, For the TSC samples sintered at, 1200  $^{\circ}\text{C}$ , 1400  $^{\circ}\text{C}$  & 1500  $^{\circ}\text{C}$  for the isothermal time 30 min & 60 min

Temp. ( $^{\circ}\text{C}$ )	$D_{v\ t=30\text{min}}$ ( $\text{m}^2/\text{s}$ )	$\ln(D_{v\ t=30\text{min}})$	$D_{v\ t=60\text{min}}$ ( $\text{m}^2/\text{s}$ )	$\ln(D_{v\ t=60\text{min}})$
1200	$4.8* 10^{-15}$	-32.9	$3.6* 10^{-15}$	-33.2
1400	$8.1* 10^{-13}$	-27.8	$6.4* 10^{-13}$	-28.1
1500	$2.1* 10^{-12}$	-26.8	$1.2* 10^{-12}$	-27.4

Table 4.8: Frequency factor ( $D_0$ ) and Activation energy estimated for various initial particle size of TSC sintered for 30 min.

Particle Size ( $\mu\text{m}$ )	$D_0$ (frequency factor) For GBD ( $\text{m}^2/\text{sec}$ )	Activation energy(kJ/mole) GBD	$D_0$ (frequency factor)( $\text{m}^2/\text{sec}$ )	Activation energy(kJ/mole) VD
8	17.2	576.8	3562.9	438.7
24	1393.8	576.8	96197.6	438.7
32	2.8	470.9	228024.9	438.7

Table 4.8: Frequency factor ( $D_0$ ) and Activation energy estimated for various initial particle size of TSC sintered for 60 min

Particle Size ( $\mu\text{m}$ )	$D_0$ (frequency factor) for GBD ( $10^{-4} \text{ m}^2/\text{sec}$ )	Activation energy (kJ/mole) GBD	$D_0$ (frequency factor) for VD ( $10^{-4} \text{ m}^2/\text{sec}$ )	Activation energy (kJ/mole) VD
8	8.1	570.2	902.8	424.6
24	654.4	570.2	24376.1	424.6
32	1.4	464.3	57778.9	424.6

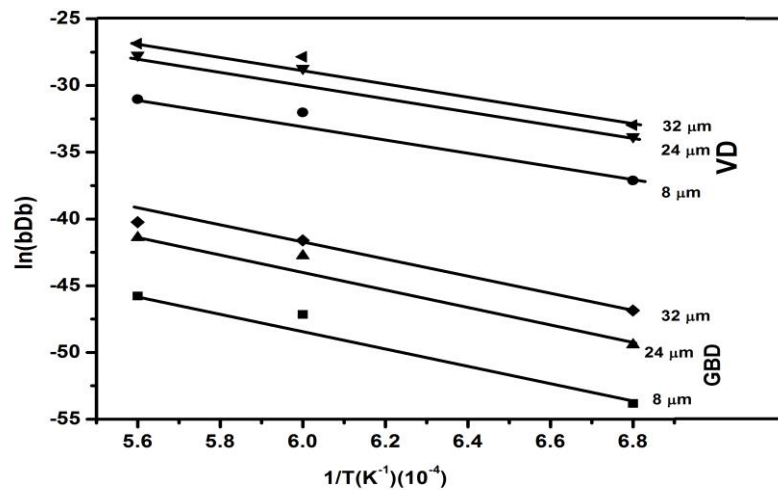


Figure 4.21: Logarithmic plots of the diffusion coefficient with respect to inverse of the temperature for particle size 8  $\mu\text{m}$ , 24  $\mu\text{m}$  & 32  $\mu\text{m}$ .

Johnson's model was used for estimation of diffusion coefficient for grain boundary diffusion and volume diffusion for samples of TSC that were heated isothermally at 1200  $^{\circ}\text{C}$ , 1400  $^{\circ}\text{C}$  & 1500  $^{\circ}\text{C}$ . It was found that activation energy to be constant as particle size increased. It was observed that as particle size increases diffusion coefficient decreases.

#### 4.4.2 Analysis of non-isothermal sintering

It was observed from dilatometer plot that onset sintering temperature was 900  $^{\circ}\text{C}$  for TSC, onset sintering temperature 1300  $^{\circ}\text{C}$  for 1Si-TSC, onset sintering temperature



1360 °C for 2Si-TSC, onset sintering temperature 1250 °C for 1Ni-TSC and onset sintering temperature 1250 °C for 2Ni-TSC. After addition of sintering aids onset sintering temperature was increased for all the samples. Non- isothermal sintering data were collected for TSC-1400 °C, TSC-1Ni-1500 °C and TSC-2Ni-1500 °C, as shown in Figures 4.22, 4.23 and 4.24 respectively. Data were collected from on-set sintering temperature point to the point where isothermal holding starts.

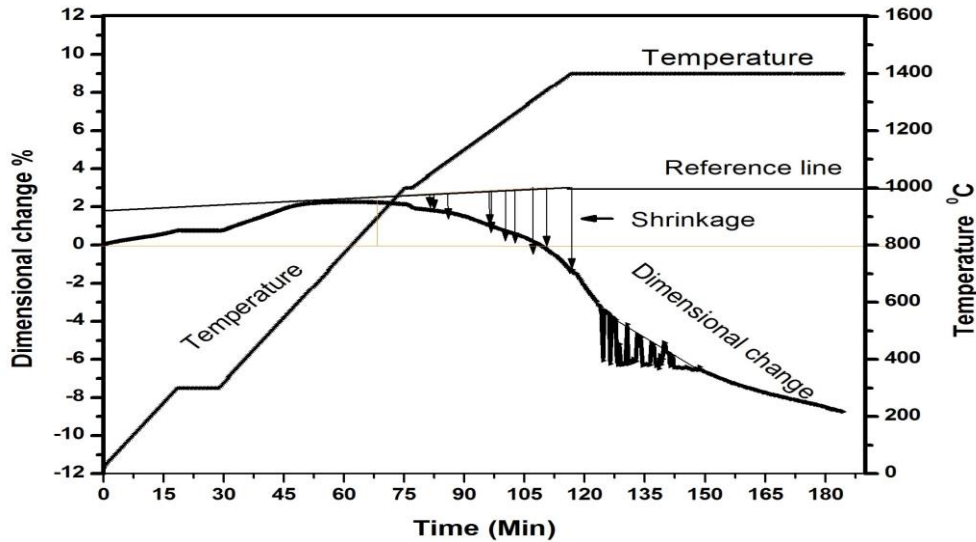


Figure 4.22: Non-isothermal shrinkage measurement for TSC sample sintered at 1400 °C

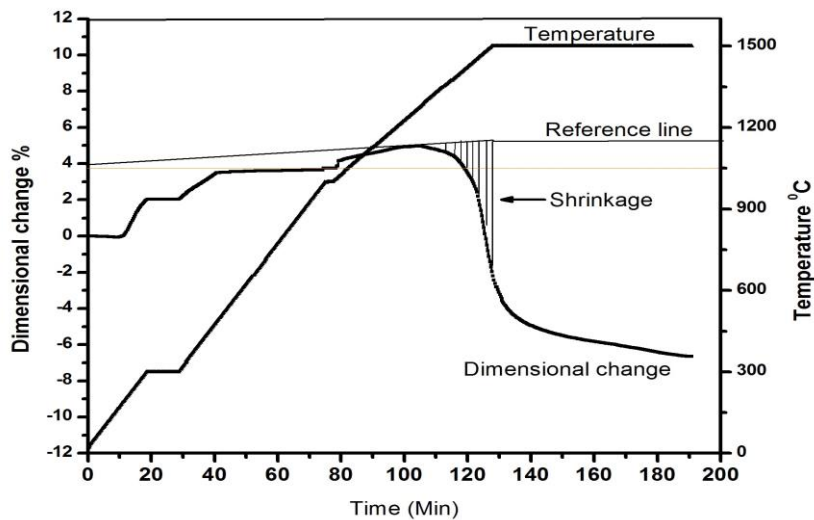


Figure 4.23: Non-isothermal shrinkage measurement for TSC-1Ni sample sintered at 1500 °C

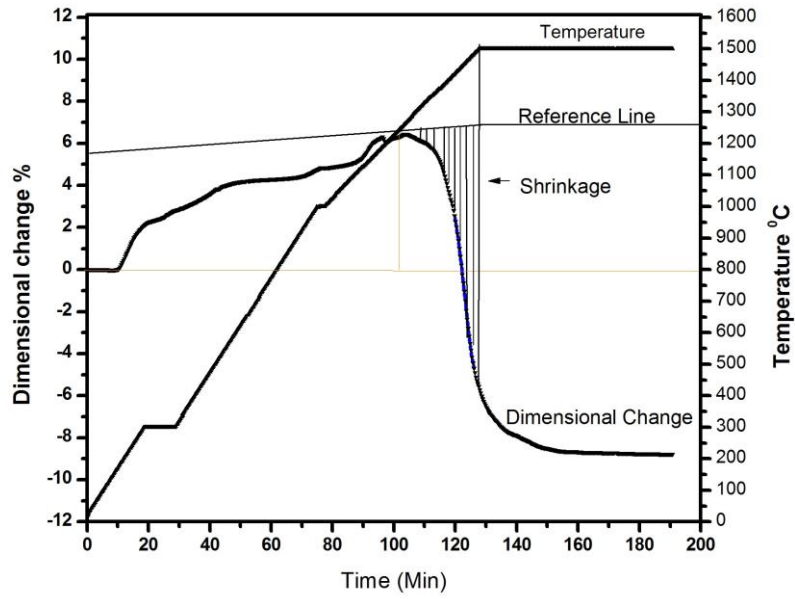


Figure 4.24: Non-isothermal shrinkage measurement for TSC-2Ni sample sintered at 1500 °C

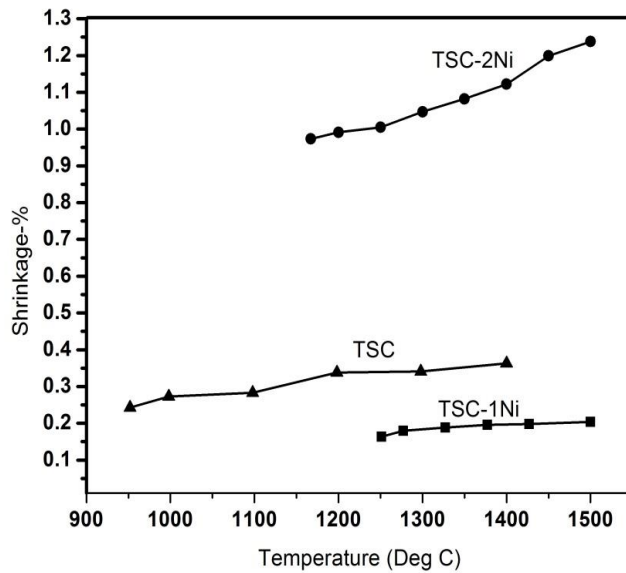


Figure 4.25: Non-isothermal shrinkage measured as a function of temperature for TSC-1400 °C, TSC-1Ni- 1500 °C and TSC-2Ni-1500 °C sample.

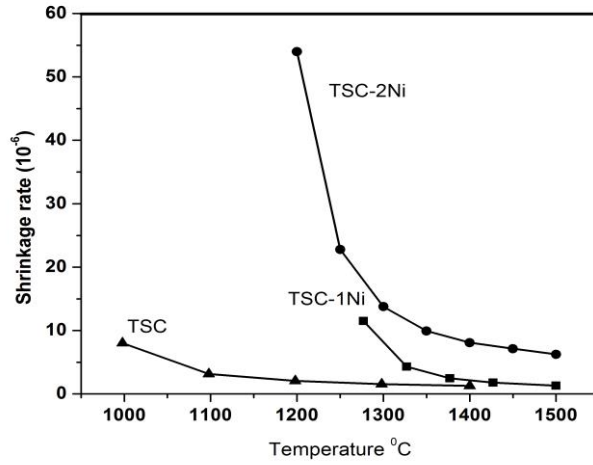


Figure 4.26: Shrinkage rate as a function of temperature measured for sintered sample, TSC-1400 °C, TSC-1Ni-1500 °C and TSC-2Ni- 1500 °C.

Figure 4.25 and 4.26, represents shrinkage and shrinkage rate with respect to temperature, 15 to 16% of shrinkage for TSC-2Ni was observed; shrinkage rate was decreases as temperature increases. For TSC-1Ni sample shrinkage was around 12 to 15% and shrinkage rate was low for TSC-1Ni.

Dilatometer data has been analyzed for non-isothermal heating of TSC-1Ni, TSC-2Ni and TSC up to 1500 °C, to understand the sintering kinetics by estimating activation energies. For analysis the data between on-set sintering temperatures to point where isothermal shrinkage starts, was considered. The activation energy (Q) was estimated using equation (5), reported for non-isothermal sintering by Han et al [19] based on Young and Cutler's equation [20].

$$\ln\left(T^p \frac{dY}{dT}\right) = -\left\{\frac{Q}{(n+1)RT}\right\} + \ln C \quad (5)$$

Where

$Y = dL_0/L_0$ ,  $dl_0$  is change in length,  $L_0 = L + dl_0$ ,

$L$ =initial length, for next temperature  $L_1 = L + dl_1$ , continued up to point where Isothermal holding starts.

T = Temperature in Kelvin,

R= Universal gas constant (8.314 Joule/mole),

C = Constant depending upon material parameters,

P has the value of 1 for viscous flow (VF), 3/2 for volume diffusion (VD) and 5/3 for GBD. The values of n are 0, 1 and 2 for VF, VD and GBD respectively. Figure 4.27, 4.28 & 4.29 show the plots based on equation (5) for estimation activation energies for TSC, TSC-1Ni & TSC-2Ni. Data were tabulated for different mechanisms (Table 4.10, 4.11& 4.12). During non-isothermal heating it was observed that, as Ni content increases, activation energy also increases.

Table 4.10: Calculated activation energy for TSC (non-isothermal)

Mechanism	Q- activation energy (kJ/mole)
Grain Boundary Diffusion	160.5
Volume Diffusion	102.9
Viscous Flow	45.4

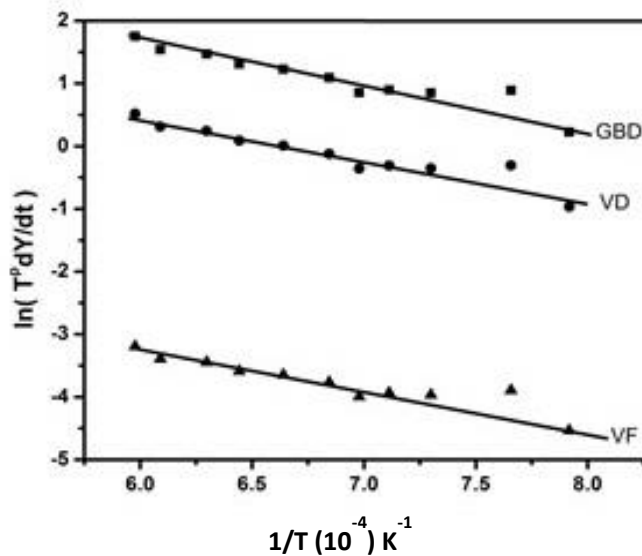


Figure 4.27: Arrhenius plots to estimate activation energies for different mechanisms for TSC- samples sintered at 1400 °C (non-isothermal)

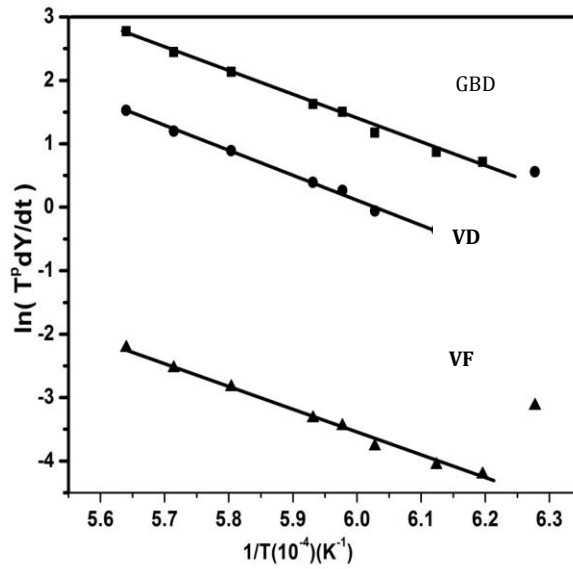


Figure 4.28: Arrhenius plots to estimate activation energies for different mechanisms for TSC-1Ni samples sintered at 1500 °C (non-isothermal)

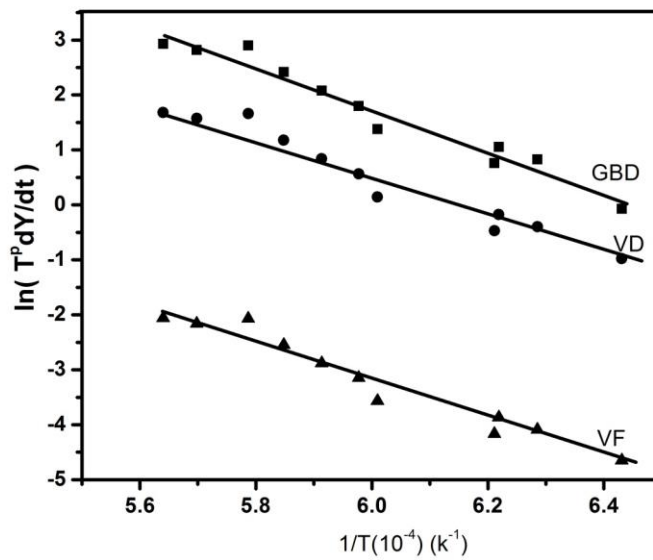


Figure 4.29: Arrhenius plots to estimate activation energies for different mechanisms for TSC-2Ni samples sintered at 1500 °C (non-isothermal heating)

Table 4.11: Calculated activation energy (Q) for TSC-1Ni-1500 °C (non-isothermal)

Mechanism	Q (kJ/mole)
Grain Boundary Diffusion	644.2
Volume Diffusion	424.8
Viscous Flow	205.4

Table 4.12: Calculated activation energy (Q) for TSC-2Ni-1500 °C (non-isothermal)

Mechanism	Q (kJ/mole)
Grain Boundary Diffusion	963.3
Volume Diffusion	602.6
Viscous Flow	294.4

## 4.5 Mechanical properties

Indentation were done on TSC and TSC-1Ni sintered samples for 2 kg and 5 kg load by using Vickers indentation test. It was observed that, indent size were significant smaller in the sample sintered with Ni additives compared to TSC samples; indicating the higher level of densification in TSC-1Ni sample [ Figures 4. 30 (a), (b), (c) & (d) ] .

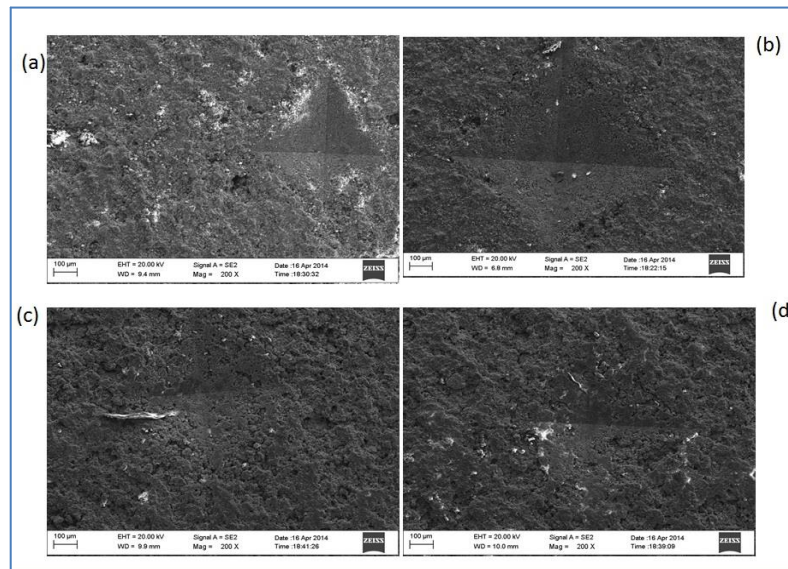


Figure 4.30 Vickers indentation test for TSC and TSC-1Ni a) 2 Kg indentation on TSC b) 5 Kg indentation on TSC c) 2 Kg indentation on TSC-1Ni & d) 5 Kg indentation on TSC-1Ni.

## Chapter 6

# Conclusions

The effect of sintering aids on sintering behavior of TSC have been studied

1. Sintering behavior of TSC powder were studied using vertical dilatometer system. Isothermal & non-isothermal sintering kinetics were analyzed, by estimating diffusion coefficients and activation energies.
2. Effect of sintering aids, such as Si & Ni on TSC powder were studied and the sintering kinetics were analyzed. Additives are found to enhance the sintered density of TSC powder. The activation energy of sintering, estimated for non-isothermal sintering, was found to be changed significantly by sintering aids.

# References

- [1] Michel W. Barsoum, “The MAX Phases: A New Class of Solids Thermodynamically Stable Nanolaminates” *Prog. Solid St. Chem.*, 28 (2000) 201-281.
- [2] Michel W. Barsoum, Miladin Radovic “Elastic and Mechanical Properties of the MAX Phases” *Annual rev. Material Res.*, 41 (2011) 195-227.
- [3] Z. M. Sun, “Progress in research and development on MAX phases: a family of a layered ternary compounds” *International Materials Reviews*, 56 (2011) 143
- [4] Michel W Barsoum, Tamel EL-Raghy, “Synthesis and characterization of a remarkable Ceramic” *Ti<sub>3</sub>SiC<sub>2</sub>*, *J. Amr. Ceram. Soc.* 79 (1996) 1953-1956
- [5] M. Magnuson, M. Palmquist, J. P. Mattesini, M. Li, S. Ahuja, R. Eriksson, and O. Jansson, “Electronic structure investigation of Ti<sub>3</sub>AlC<sub>2</sub>, Ti<sub>3</sub>SiC<sub>2</sub>, and Ti<sub>3</sub>GeC<sub>2</sub> by soft x-ray emission spectroscopy” *Physical review*, 72 (2005) 245101-1-9.
- [6] M. Radovica, M. W. Barsoum, T. El-Raghy, S. M. Wiederhorn, W. E. Luecke. “Effect of temperature, strain rate and grain size on the mechanical response of Ti<sub>3</sub>SiC<sub>2</sub> in tension” *Acta Materialia* 50 (2002) 1297-1306.
- [7] Mohamad Johari Abu, Julie Juliewatty Mohamed, Zainal Arifin Ahmad, “Effect of Excess Silicon on the Formation of Ti<sub>3</sub>SiC<sub>2</sub> Using Free Ti/Si/C Powders Synthesized via Arc Melting” *ISRN Ceramics*, 10 (2012) 5402.
- [8] Radhakrishnan R, Bhaduri SB, Henager Jr CH, “Analysis on the sequence of formation of Ti<sub>3</sub>SiC<sub>2</sub> and Ti<sub>3</sub>SiC<sub>2</sub>/SiC composites” *Adv Powder Metall Part Mater* 13 (1995) 129–137.
- [9] B. B. Panigrahi, M. C. Chu, A. Balakrishnan, S. J. Cho, “Synthesis, pressureless densification and sintering kinetics of Ti<sub>3</sub>SiC<sub>2</sub> powder” *J. Mater. Research*, 24 (2009) 487-492.
- [10] Z. M. Sun, S. Yang, H. Hashimoto, “Effect of Al on the synthesis of Ti<sub>3</sub>SiC<sub>2</sub> by reactively sintering Ti–SiC–C powder mixtures” *Journal of Alloys and Compounds* 439 (2007) 321–325.
- [11] K. Tang, C. Wang, L. Wu, X. Guo, X. Xu, and Y. Huang, “Sintering of Ti<sub>3</sub>SiC<sub>2</sub> with B<sub>2</sub>O<sub>3</sub> additions” *Ceram. Int.*, 28 (2002) 761.



- [12] B. B. Panigrahi, N. S. Reddy, A. Balakrishnan, M-C Chu, S-J Cho, J. J. Gracio, "Nickel assisted sintering of  $\text{Ti}_3\text{SiC}_2$  powder under pressureless conditions" *J. Alloys and Compounds*, 505 (2010) 337-342.
- [13] Li SB, Xie JX, Zhang LT, Cheng LF. "Synthesis and some properties of  $\text{Ti}_3\text{SiC}_2$  by hot pressing of titanium, silicon and carbon powders part 1-effect of starting composition on formation of  $\text{Ti}_3\text{SiC}_2$  and observation of  $\text{Ti}_3\text{SiC}_2$  crystal morphology" *Mater Sci Technology*, 19 (2003) 1442–1446.
- [14] P. Aguiar, C. S. Adjiman, and N. P. Brandon, "Anode-supported intermediate temperature direct internal reforming solid oxide fuel cell. I: model-based steady-state performance" *J. Power Sources*, 138 (2004) 120–136.
- [15] Racault C, Langlais F, Naslain R. "Solid-state synthesis and characterization of ternary phase  $\text{Ti}_3\text{SiC}_2$ " *J. Mater Sci.*, 29 (1994) 3384–3392.
- [16] N.F. Gao, J.T. Li, D. Zhang, and Y. Miyamoto, "Rapid synthesis of dense  $\text{Ti}_3\text{SiC}_2$  by spark plasma sintering" *J. Eur. Ceram.*, 22 (2002) 2365.
- [17] S. Yang, Z.M. Sun, and H. Hashimoto, "Formation of  $\text{Ti}_3\text{SiC}_2$  from Ti–Si–TiC powders by pulse discharge sintering (PDS) technique". *Mater. Res. Innovat.*, 7 (2003) 225.
- [18] C.L. Yeh and Y.G. Shen, "Effects of TiC addition on formation of  $\text{Ti}_3\text{SiC}_2$  by self-propagating high-temperature synthesis" *J. Alloys Compd.* 458 (2008) 286.
- [19] J. Han, A. M. R. Senos, P. Q. Mantas, "Nonisothermal sintering of Mn doped ZnO" *J. Eur. Ceram. Soc.* 19 (1999) 1003.
- [20] W. S. Young, I. B. Cutler "Initial sintering with constant rate heating" *J. Am. Ceram. Soc.* 53 (1970) 659.
- [21] El-Raghy T, Barsoum MW, Zavaliangos A, Kalidindi SR "Processing and mechanical properties of  $\text{Ti}_3\text{SiC}_2$ . II. Effect of grain size and deformation temperature" *J. Am. Ceram. Soc.* 82 (1999) 2855–60.
- [22] Gilbert CJ, Bloyer DR, Barsoum MW, El-Raghy T, Tomsia AP, Ritchie RO "Fatigue-crack growth and fracture properties of coarse and fine-grained  $\text{Ti}_3\text{SiC}_2$ " *Scr. Mater.* 238 (2000) 761–67.
- [23] C. W. Corti, "Sintering Aids in Powder Metallurgy, the role of the platinum metals in the activated sintering of refractory metals" *Platinum metals rev.* 30 (1986) 61.

- [24] A. K. Khanra and M. M. Godkhindi, "Effect of Ni additives on sintering behavior of SHS ZrB<sub>2</sub>" *Adv. App. Ceramics*. 104 (2005) 273-276.
- [25] Thummler. F., "Introduction to Powder Metallurgy".
- [26] M. W. Barsoum, D. Brodtkin and El-Raghy "layered machinable ceramics for high temperature applications" *Scripta material* 36 (1997) 355.
- [27] Y. Zou, Z-M Sun, H. Hashimoto and S. Tada, "Synthesis of Ti<sub>3</sub>SiC<sub>2</sub> through pulse Discharge Sintering of powder mixture containing coarse Ti" *Materials Transactions*, 47 (2006) 1910-1913.
- [28] Z. F. Zhang, Z-M. Sun, H Hashimoto and T Abe, "Application of pulse discharge sintering (PDS) technique to rapid synthesis Ti<sub>3</sub>SiC<sub>2</sub> from Ti/Si/C powders" *Journal of European Ceramic Society* 22 (2002) 2957-2961.
- [29] J-F Li, F Sato, R Watanabe, "Synthesis of Ti<sub>3</sub>SiC<sub>2</sub> polycrystals by HIP of the elemental powders" *J. materials science letters* 18 (1999) 1595-1597.
- [30] El-Raghy T, Barsoum MW, Zavaliangos A, Kalidindi SR., "Processing and mechanical properties of Ti<sub>3</sub>SiC<sub>2</sub>. II. Effect of grain size and deformation temperature" *J. Am. Ceram. Soc.* 82 (1999) 2855–60.
- [31] N. F. GAO et al, Dense "Ti<sub>3</sub>SiC<sub>2</sub> prepared by reactive HIP" *J. material science* 25 (1999) 4385-43
- [32] El Saeed, M. A., Deorsola, F. A., & Rashad, R. M., "Optimization of the TSC MAX phase synthesis. *International Journal of Refractory Metals and Hard Materials*" 35 (2012) 127-131.
- [33] Zhen, T., Barsoum, M. W., & Kalidindi, S. R. "Effects of temperature, strain rate and grain size on the compressive properties of TSC" *Acta materialia*, 53 (2005) 4163-4171.
- [34] Ke Tang, C Wang, Y Huang, Q Zan, Xingli Xu, "A study on the reaction mechanism and growth of Ti<sub>3</sub>SiC<sub>2</sub> synthesized by hot-pressing" *Materials Science and Engineering*, 28 (2002) 206–212.
- [35] Debashis Bandyopadhyay, "The Ti-Si-C System" *JPEDAV* 25 (2004) 415-420.
- [36] B. B. Panigrahi, "Prediction of Diffusion Coefficient of Ti<sub>3</sub>SiC<sub>2</sub> and Cr<sub>2</sub>AlC Ceramics Using Sintering Models" *Transaction of Powder Metallurgy Association of India* 38 (2012) 71-75.